Results: 11 patients had multiple CA of the same histologic type in the same lobe (stage IIIB) and 1 patient had CA involving different ipsilateral lobes and positive subcarinal lymph node (stage IV). By molecular analysis, 5/12 CA were classified as metastases, including the 1 CA in different lobes. These metastatic CA would have the same original stage. However, 7/12 CA were re-classified as de novo by molecular analysis, therefore each CA should have a separate T classification instead of being classified as T4 for both CA. After reclassification, 7 patients were staged as follows: IA (2 patients), IB (3 patients), and IIB (2 patients)

Conclusions: Molecular analysis downstaged 7/12 (58%) patients with multiple lung tumors involving the same lobe by demonstrating that they are de novo tumors and not metastases, which has prognostic implications. We believe that when multiple lung carcinomas of same histologic type are encountered, molecular analysis may contribute to a more acurate TNM staging. In our series 7/12 (58%) patients would need an ammended TNM classification in the surgical pathology report.

1510 MISFISHIE: A Specification for Reporting Immunohistochemical Findings. Assessment of Compliance in Publications

LD True, EW Deutsch, D Campbell, L Pascal, AJ Oudes, AY Liu. University of Washington, Seattle, WA; Institute for Systems Biology, Seattle, WA.

Background: A goal of the biomedical literature is to report results in sufficient detail so that the study can be independently replicated. To ensure that a sufficient level of detail is provided, a minimum information specification is needed for reporting data. A data content specification has already been widely accepted by the microarray community - MIAME. However, no specification exists for immunohistochemistry experiments. In this study, we developed and evaluated a specification for immunohistochemical studies. This specification details the minimum information that should be provided when reporting immunohistochemistry experiments. Compliance to this standard should provide other investigators enough information to reproduce the experiments and/or to evaluate data upon which results are based.

Design: A specification that consists of 6 sections – Design (e.g. number of cases, number of stains), Processing (e.g. tissue type, fixative), Antibody Data, Staining Protocol, Imaging Data , and Image Characterization (e.g. method of image evaluation) - was developed. This specification does not dictate a specific format for data reporting. A selection of immunohistochemistry articles from the past 5 years reporting studies was assessed for compliance with the six sections of the specification. Each reviewer assessed each of 32 assigned articles. Compliance for each MISFISHIE subsection was rated on a scale of 0 to 10. Score of 10 indicates that all information the reviewer needed to reproduce the experiment was provided; scores <10 correspond to how incomplete the information was that the reviewer thought necessary to reproduce the work. Scores of 8 and 9 were considered a low pass, e.g. the reviewer could reproduce the experiment with only a few assumptions.

Results: Of the papers, only 4 (13%) were deemed MISFISHIE compliant in all sections. 28% were out of compliance in only one section. 31% did not comply in two sections. More than 90% complied with sections on Design and Specimen Processing. 75% complied with sections on Antibody Information and Staining Protocol. Only 16% of articles were compliant with Section 5 (Imaging Data).

Conclusions: Many papers lack sufficient detail for independent investigators to reproduce the studies with complete confidence. We propose that investigators and journal editors evaluate immunohistochemical studies using the MISFISHIE specification.

1511 High-Throughput Image Analysis of Tissue Microarrays Based on a Public Domain Software Program

DA Turbin, AKW Chan, MCU Cheang, DG Huntsman, CB Gilks, TO Nielsen, CB Gilks. Prostate Research Centre at the Vancouver General Hospital, British Columbia Cancer Agency and University of British Columbia, Vancouver, BC, Canada.

Background: Visual assessment of IHC staining of TMA can be time-consuming and laborious. Several companies offer TMA-scanning platforms with image-analysis software; however, these are hardware-specific and expensive.

Design: We created Java-based software for the public domain image analysis program, ImageJ (http://rsb.info.nih.gob/ij/). This plugin utilizes a novel algorithm for nuclear IHC staining analysis. It performs colour deconvolution (G. Landini) and works separately with the DAB and hematoxylin channels. Thresholding can be manual or automatic. A watershed algorithm separates touching objects. Multiple parameters of the segmented objects are then analysed, including area, Feret's diameter, circularity, and roundness. Texture analysis is performed using the 21 parameters as described in R. Haralick et al., 1983. Those objects that do not meet the tumor cell criteria are excluded. The output file presents percent of positive nuclei, percent of positive area, optical density of positive objects, and a number of other features. The program saves result images showing positive and negative nuclei outlined by different colors, thereby allowing visual quality control of tumor nuclei identification.

Results: The plugin was tested on breast TMA containing 4648 tissue cores, stained for ER (clones SP1 and 1D5), Ki67, and p53. Visual examination of the output images shows that our program allows accurate selection of positive and negative tumor nuclei. The programme does not make any assumptions about the average size or shape of tumor cells, allowing parallel analysis of pleomorphic tumors with usual ductal and lobular carcinomas. Texture analysis filters out the majority of lymphocytes and stromal cell nuclei, greatly increasing the accuracy of tumor cell identification. ER staining was positive in 66.14% using the SP1 antibody, and 62.11% for 1D5. Percent of positive tumor nuclei in ER staining is associated with better disease specific survival (p = 2.4E-06), and in Ki67 (p = 7.6E-016) and p53 (p = 9.36E-012) with worse survival, as determined by univariate Cox regression analysis.

Conclusions: We developed a robust image analysis programme specifically designed for nuclear staining analysis of IHC slides, whether TMA or whole section. This freeware provides quantitative scoring of nuclear immunostaining digital images.

1512 A Proposal for Improved Quality Assurance in Flow Cytometry Using the Rmax Statistic for Kappa-Lambda Testing

Q Xie, P Bhattacharyya, H Xu, D Xu, M Pathan, Q Hu, F Sen, J Bang, X Xue, H Ratech. Montefiore Med Ctr, Bronx, NY; Hackensack U Med Ctr, Hackensack, NJ; Boston U Med Ctr, Boston, MA; Creighton U Med Ctr, Omaha, NE; New York U Med Crt, New York, NY; Albert Einstein Coll Med, Bronx, NY.

Background: Flow cytometric analysis of percent κ and λ surface immunoglobulin (sIg) light chains is important for determining B-cell clonality. However, it has been problematic to compare data within one laboratory over time or among different laboratories because there is no generally agreed upon statistical approach.

Design: For evaluating sIg light chain restriction, we transformed all κ / λ ratios to maximum ratios. That is, Rmax=max (κ / λ, λ / κ), so that all resulting ratios were at least 1. Percent κ and λ lymph node data were obtained from four medical centers during 2002, 2003, and 2004. Both inter-institutional differences and year-to-year variations in optimal Rmax statistic cut-off value and in sensitivity and specificity of the same R-max cut off value were analyzed.

Results: 938 κ, λ data pairs from four institutions were converted to maximum ratios. The Rmax cut-off values were chosen to optimally separate reactive lymphoid hyperplasia from B-cell lymphoma. To compare the sensitivity and specificity across years and sites, a cut-off value of 2.84 was used. A separate logistic regression was used for sensitivity and specificity with institution, year and their interaction as covariates. The results show that there were no interaction effects between sites and years. However, within each site, there was variation in sensitivity across years (p=0.0090), but for a given year there was no variation in sensitivity between sites (p=0.1023). No statistically significant difference was found in specificity across years and between sites.

Site	Year	N	Rmax cut-off value	Sensitivity	Specificity
1	02	100	2.84	0.95	0.92
	03	85	3.01	0.95	0.94
	04	111	2.84	0.96	0.94
2	02	87	2.50	0.96	0.76
	03	93	2.84	0.97	0.92
	04	110	2.50	0.98	0.82
3	02	59	3.33	1.00	0.85
	03	78	2.84	1.00	0.85
	04	90	2.33	0.97	0.90
4	02	21	2.84	1.00	0.86
	03	45	2.84	1.00	0.93
	04	59	2.84	0.95	0.97

Conclusions: We propose that the Rmax statistic, which can reveal previously unsuspected variations in κ, λ data, may improve quality assurance within a single facility over time and may promote sharing of data among institutions.

Techniques

1513 Real-Time Region-of-Interest-Based Image Database Query and Differential Diagnosis Generation Utilizing Third-Generation Vector Quantization Techniques in Concert with N-Space Voronoi Mapping

UJ Balis. Massachusetts General Hospital and Harvard Medical School, Boston, MA.

Background: The advent of whole slide digital imaging allows for exploration of histologic datasets by automated methods for determination of similarity with prior stored images. Additionally, if established image repositories are pre-coordinated with diagnostic data, as linked metadata, there exists the opportunity to construct region-of-interest-based query tools, that use image content itself (and not text) as the predicate for carrying out searches.

Design: An image query and retrieval engine was constructed using C++ 6.0 (Microsoft Corporation, Redmond, WA) as the development environment for the 3rd generation Vector Quantization Discovery Toolset (VQDT) already in place at the MGH Pathology Digital Imaging Laboratory. This system consists of an N-space Sparse Matrix mapping system, an advanced Voronoi projective filter for carrying out principle component analysis (PCA), a Voronoi Visualization tool suite and a highly-optimized VQDT Bayesian Inference matching filter to provide for real-time matching of predicate regions of interest with established vocabularies and associated diagnostic metadata.

Results: Histologic digital imagery content was acquired from 157 different slides and subsequently parsed through the VQDT in training mode, allowing for generation of a general class of VQ principle-component elements (vectors) spanning eight organ systems. Of each organ system selected, baseline "normal histology" cases were included in addition to histopathologic entities. Submitted imagery was tagged with pre-coordinated diagnostic data, allowing for spatially-tagged vocabulary metadata. An additional 25 wide-field slides were scanned with their content used as the predicate for testing of the specificity and sensitivity of the N-space VQ inference engine. This was carried out by selecting diagnostically archetypal regions of interest from these 25 images for query against the established vocabulary. Resultant Bayesian clusters of vectors returned from the Voronoi mapping were evaluated in terms of their confidence intervals for returning one or more tagged diagnoses which correlated with the objectively deemed diagnoses of the test set. Resultant sensitivity and specificity for the test set was 93% and 97% respectively.

Conclusions: Vector Quantization with N-Space Voronio mapping demonstrates utility in providing for satisfactory sensitivity and specificity as an automated image matching and differential diagnosis generation tool.

1514 Virtual Mitosis Recognition through Digital Algorithms Improves and Standardizes Mitotic Counting in Diverse Human Neoplasms
SH Barsky, A Josi, A Deshpande, S Keyhani-Rofagha, NJ Karlin, AS Gholap. The Ohio State University College of Medicine, Columbus, OH; Olive View, Sylmar, CA; BioImagene, Inc, San Mateo, CA.
Background: Pathologists routinely quantify mitotic figures. The mitotic count is a measure of proliferation and is both a prognostic as well as predictive marker in diverse tumors. Mitosis detection is very subjective because necrotic / apoptotic nuclei can resemble mitotic figures. Intraobserver, interobserver and fatigue variability also contribute to inaccuracy. For these reasons objective measurements of proliferation such as S phase and Ki-67 have supplanted "mitosis counts" yet such measurements are only surrogates for true cell division.
Design: Since microscopic images can be scanned and digitized through virtual microscopy, we wondered whether interpretative computer algorithms could be written that would accurately quantitate mitosis in diverse human neoplasms. We used prototype human tumoral xenografts and their wide gamut of mitotic figures to create mitotic templates based on nuclear threshold, size and shape. These templates were refined using a neural network approach to distinguish mitotic figures from apoptotic / necrotic nuclei. These refinements were based on the nuclear aspect ratio (the ratio of major / minor axis) and the ratio of the nuclear perimeter / area.
Results: We applied these algorithms to 25 sarcomas (5 leiomyosarcomas, MFHs, chondrosarcomas, rhabdomyosarcomas, liposarcomas); 15 pulmonary carcinoids (5 malignant, atypical and benign) and 10 breast carcinomas of varying grade. Previously written tumor-specific recognition algorithms could effectively filter out the non-neoplastic regions and allow mitotic counting of only the tumor areas. In all tumors, mitosis could be accurately counted with a false positive rate of 10% and a false negative rate of 5% compared to manual interpretation. However the automated mitotic measurements showed no intraobserver, interobserver or fatigue variability and could be made in seconds over the entire scanned slide, thereby saving the pathologist hours of tedium and eliminating the conventional 10 H.P.F.s sample bias.
Conclusions: Digital image algorithms allow for accurate determination of mitosis on virtual slides of diverse human neoplasms where accurate mitotic counting is important. Because of its objectivity, reproducibility and speed, virtual mitosis recognition will assist the pathologist by providing an improved proliferation measurement over manual counting, S phase or Ki-67 determinations.

1515 Evaluation of EGFR Expression in Colorectal Carcinomas, Adenomas, and Normal Mucosa: A Comparison between Two Commonly Used Antibodies
R Bhargava, B Chen, DS Klimstra, C Hedvat, L Tang, W Gerald, J Teruya-Feldstein, J Shia. Magee-Womens Hospital of University of Pittsburgh Medical Center, Pittsburgh, PA; Memorial Sloan Kettering Cancer Center, New York, NY.
Background: Anti-epidermal growth factor receptor (EGFR) therapy for colo-rectal carcinomas currently requires evaluation of EGFR expression within the tumor tissue. No comparative studies on the performance of two most commonly used antibodies are currently available.
Design: Seven hundred and forty-four tissue microarray core samples from 248 cases of primary and metastatic colorectal carcinomas, colorectal adenomas, and normal colorectal mucosa were evaluated with pharmDx kit (DAKO, Carpinteria, CA) and 31G7 (Ventana Inc., Tucson, AZ) EGFR monoclonal antibodies. Staining intensity between the two stains was compared using an automated image analysis system (ACIS II, ChromaVision Medical Systems, Inc., San Juan Capistrano, CA). The intensity of positive staining (brown color) was measured on a scale of 0-255.The staining intensity was also scored manually as 0, 1+, 2+ and 3+.
Results: The Dako antibody stained the cells slightly more intense than the Ventana antibody; however, the median staining intensities scored by the ACIS II between the two antibodies were not significantly different statistically. A linear correlation was obtained between ACIS scores and manual scoring categories. The median ACIS intensity scores for the four manual scoring categories with the Dako antibody were as follows: 0: 67.5, 1+: 75.5, 2+: 89.6, and 3+: 106. The median ACIS intensity scores for the four manual scoring categories with the Ventana antibody were as follows: 0: 71.3, 1+: 73.6, 2+: 84.6, and 3+: 99.1. The classification of tumors as EGFR-negative (0+) or positive (1+, 2+ or 3+) was concordant in 151 of 160 (94.4%) carcinomas with two antibodies using manual scoring.

Correlation of manual grading between Dako antibody and Ventana antibody in colonic adenocarcinomas.

	Dako 0	Dako 1+	Dako 2+	Dako 3+	Total
Ventana 0	17	5	0	0	22
Ventana 1+	4	53	35	1	93
Ventana 2+	0	0	24	13	37
Ventana 3+	0	0	0	8	8
Total	21	58	59	22	160

p value<0.0001 (p value calculated after combining 2+ and 3+ categories)
Conclusions: The EGFR expression results are comparable as obtained by immunohistochemistry using the EGFR pharmaDx kit from Dako and the 31G7 clone from Ventana. Either antibody may be used for immunohistochemical detection of EGFR in colorectal carcinomas. In addition, manual scoring has an excellent correlation with automated scoring.

1516 Comparison of Dako EGFR pharmDx Kit and Zymed Antibody for the Assessment of EGFR Status in Colorectal Adenocarcinoma
AF Buckley, S Kakar. UCSF and VA Medical Center, San Francisco, CA.
Background: Many colorectal cancers overexpress epidermal growth factor receptor (EGFR) and are targets for therapy with anti-EGFR agents like Erbitux. Immunohistochemistry has been advocated for determining the EGFR status in colorectal cancer. However, there is scarce objective data on comparison of EGFR antibodies from different commercial sources.

Design: Formalin-fixed, paraffin-embedded tissue from 30 cases of colorectal cancer (19 primary, 11 metastatic) was analyzed for EGFR expression using two monoclonal antibodies: Clone 2-18C9 (Dako, Carpinteria, CA) and Clone 31G7 (Zymed Laboratories, South San Francisco, CA). For the Dako antibody, the EGFR pharmDx kit was used as per the manufacturer's instructions. For the Zymed antibody, the sections were deparaffinized, hydrated through graded alcohols and treated with 3% H_2O_2 to block endogenous peroxidase activity. Antigen retrieval was performed by incubation with 0.4% pepsin at 42°C for 12 minutes followed by application of primary antibody (1:300) for 30 minutes. The detection was performed using the Dako Envision Plus system (Dako, Carpinteria, CA). The cases were scored as positive when more than 1% of tumor cells showed cell membrane staining based on the FDA-approved criterion. The cost of the two procedures was determined.
Results: EGFR expression was seen in 16 (53%) of cases (11 primary, 5 metastatic) with the Dako pharmDx kit. The Zymed antibody showed positive results in 19 (63.3%) cases (13 primary, 6 metastatic). The cost per case with the Dako EGFR pharmDx kit was $40 (50 tests per kit that costs $2000). The cost per case with the Zymed antibody was $12.35 ($4.35 for antibody + $8.00 for reagents).
Conclusions: The Zymed antibody is more sensitive in detecting EGFR expression in colorectal cancer, detecting 10% more cases compared to the Dako EGFR pharmDx kit. Although the Dako EGFR pharmDx kit is FDA approved, it is three times more expensive and appears to have lower sensitivity. The use of Zymed antibody can increase the number of patients that would qualify for use of anti-EGFR agents.

1517 Comparison of Two Different PCR Protocols for Detection of t(14;18) in Follicular Lymphomas
M Cankovic, R Hawley, L Whiteley, K Gu, RJ Zarbo. Henry Ford Hospital, Detroit, MI.
Background: The t(14;18) is present in 70 to 90% of follicular lymphomas (FL). Detection of t(14;18) can be utilized to diagnose and monitor FL. Conventional cytogenetic analysis, fluorescent in situ hybridization (FISH), Southern blot analysis, and polymerase chain reaction (PCR)-based assays are established detection techniques. Depending on the strategy employed, PCR-based assays can detect t(14;18) in up 70% of FL. In this study, we sought to determine the sensitivity of two different PCR protocols for detection of t(14;18) in FL in formalin-fixed paraffin-embedded tissue.
Design: 50 cases of FL and 10 cases of reactive lymphoid hyperplasia were studied; excisional lymph node biopsies were utilized in all cases. The FL were histologically and, in most cases, immunophenotypically defined; all had a predominantly follicular infiltrative pattern. Sections were cut from formalin-fixed paraffin-embedded tissue blocks, and QIAamp DNA mini kit (Qiagen) was used for DNA isolation. Two different protocols were used for t(14;18) detection: 1) Dual labeled TaqMan protocol for detection of MBR breakpoints by quantitative real time PCR (QPCR) and 2) bcl2/JH translocation assay (In Vivo Scribe) for detection of MBR and mcr breakpoints by multiplex PCR and capillary electrophoresis (ABI 3100, Applied Biosystems).
Results: Rearrangements involving MBR were detected by QPCR in 32 FL cases (64%), and by multiplex PCR/capillary electrophoresis (PCR/CE) in 26 cases (52%). Rearrangements involving mcr were detected by PCR/CE in 6 cases (12%). Rearrangements involving MBR or mcr were not detected by either QPCR or PCR/CE in 9 of the 10 cases of reactive lymphoid hyperplasia. A rearrangement involving MBR was found at low level by both QPCR and PCR/CE in 1 of the 10 control cases.
Conclusions: Our results indicate that both QPCR and PCR/CE can effectively detect the t(14;18) in formalin-fixed paraffin embedded tissue in the majority of cases of FL. The detection rate was 64% with each protocol.

1518 Evaluation of Different DNA Extraction Methods in Archival Heart Tissue for Postmortem Mutational Analysis
E Carturan, DJ Tester, G Thiene, MJ Ackerman. University of Padua Medical School, Padua, Italy; Mayo Clinic College of Medicine, Rochester, MN.
Background: Five to ten percent of all sudden deaths remain unexplained. Postmortem genetic testing is often desired. However, paraffin-embedded tissue (PET) is typically the only source of DNA available. This study aims to compare different DNA extraction procedures and to develop the most efficient method for obtaining DNA from PET, to be used for postmortem mutational analysis.
Design: We compared 26 permutations involving 2 different deparaffination methods (microwave vs xylene), 5 commercial kits (Ex Wax-Chemicon, MagneSil-Promega, Nucleon HT-Amesham Biosciences, Puragene-Gentra Systems, QIAamp-Qiagen), and 8 standard laboratory based methods that involved one of two different digestion methods (Proteinase K overnight or sonication) and one of four different purification steps (boiling, DNAzol-Invitrogen, Instagene-Biorad, or phenol/chloroform). Initially, PCR amplification of 4 amplicons (199 bp to 300 bp) was evaluated using all 26 permutations on 3 different PET blocks. Using the best protocol determined from this primary evaluation, the ability to analyze 30 amplicons (194-349 bp) from DNA derived from 11 PET blocks was examined.
Results: Overall, there was no difference in either deparaffination method in terms of efficacy in the extraction and amplification of DNA (xylene 62/156, microwave 68/156, ns). However, when using microwave deparaffination, overnight digestion with Proteinase-K was superior to sonication (25/48 vs 10/48, p < 0.003). Although there was significant variability between the 8 standard laboratory-based methods, the commercial kits provided a greater overall yield of analyzable DNA (68/120 vs 53/192, p = 0.001). Among the commercial kits, Nucleon HT generated the lowest yield (23/88, 26%) of analyzable DNA compared to Ex Wax (41/88), QIAmp (43/88), Puragene (46/88), and MagneSil (55/88, 62%, p < 0.008). Using the best hybrid protocol, an average of 19 ± 10 of the 30 amplicons was analyzable from the 11 PET blocks (range 0 to 29 amplicons).
Conclusions: Although PET can be utilized as a source for conducting a molecular autopsy in historical sudden unexplained death (SUD) cases, a comprehensive

surveillance of possible SUD-associated genes will be limited. Given these challenges and shortcomings, it is advised that the standard SUD postmortem evaluation include archiving either EDTA-preserved blood or frozen tissue to facilitate postmortem genetic testing.

1519 Oligodendroglial Versus Astrocytic Tumors: A Pilot DNA Microarray Study on Formalin-Fixed Paraffin-Embedded Tissues
Y-T Chen, J Kao, AD Polydorides, E Lavi. Weill Medical College of Cornell University, New York, NY.
Background: The differential diagnosis between oligodendroglial and astrocytic tumors is clinically crucial but histologically challenging, particularly in high-grade or mixed lesions. Recent studies have indicated that various types and grades of gliomas may be distinguishable by DNA microarray analysis. To extend these studies and test the potential utility in diagnostic pathology, we initiated a pilot study using formalin-fixed paraffin-embedded (FFPE) tumor tissues.
Design: Seven cases each of astrocytic and oligodendroglial tumors of various histological grades were selected and one representative FFPE block was used to extract RNA and perform microarray analysis, using reagents designed for the analysis of FFPE tissues (Ambion Optimum FFPE RNA extraction kit, Arcturus ParadiseTM reagent and Affymetrix X3P chip).
Results: Sufficient RNA yield was obtained from all cases, all amplifiable by quantitative RT-PCR assay of 18S RNA and GAPDH (Glyceraldehyde-3-phosphate dehydrogenase) endogenous controls. The RNA quality, however, was highly variable. Three cases with the best RNA quality were selected from each group for two-cycle amplification to prepare cRNA. Five yielded sufficient cRNA for the microarray assay. One case, of the worst RNA quality among this group of six, yielded insufficient cRNA. Evaluation of the microarray data showed that positive hybridization signals ("present call") varied between 8-15% in 4 samples and 31% in 1 sample, substantially lower than routinely obtained with fresh-frozen tissues (30-60%). Unsupervised hierarchical clustering was attempted on the 4 samples with lower present-calls, as the exceptional high present-call in the last case would automatically segregate it from the other cases. Results showed that the 2 astrocytic tumors clustered separately from the 2 oligodendroglial tumors, with 412 genes showing differential expression (>2 fold change, ANOVA p<0.01). Most of the top ranking genes on the list were unknown genes, and their significance remains to be validated.
Conclusions: RNA quality from FFPE tissues was highly variable and only some could be used for microarray analysis. The microarray data was significantly inferior to that derived from fresh tissues. Although preliminary results showed astrocytic tumors to cluster separately from oligodendroglial tumors, these results need to be interpreted with great caution. Additional experiments are warranted to further assess the value and limitations of gene profiling using FFPE tissues.

1520 Clinical Validation of Two PCR-Based Assays for Detection of the *JAK2*V617F Mutation in Non-CML Chronic Myeloproliferative Disorders
MS Clark, SG Fuller, JA DiGiuseppe. Hartford Hospital, Hartford, CT.
Background: A V617F mutation in the nonreceptor tyrosine kinase *JAK2* is detectable in most cases of polycythemia vera (PV), and in a significant proportion of cases of essential thrombocythemia (ET) and chronic idiopathic myelofibrosis (CIMF). However, a systematic evaluation of assays potentially suitable for use in the clinical molecular diagnostics laboratory has not been reported.
Design: Allele-specific PCR (AS-PCR) and PCR-RFLP assays (Baxter EJ, et al. *Lancet* 2005;365:1054-1061) were performed using DNA extracted from fresh peripheral blood (PB) and bone marrow (BM) specimens, archival paraffin-embedded BM aspirate clot specimens, and archival BM aspirate smears (in the latter case, using the Pinpoint Slide DNA Isolation System, Zymo Research).
Results: A *JAK2* (V617F) mutation was detected in 23 of 25 (92%) cases of PV, 5 of 11 (45%) cases of ET, and 1 of 2 (50%) cases of CIMF. Mutations were also detected in 10 of 11 (91%) cases of non-CML chronic myeloproliferative disorders (CMPDs) NOS, and in 4 of 6 (67%) cases in which unequivocal distinction between a CMPD and a reactive process was not possible solely on the basis of the pathologic findings. No mutations were detected in any of 9 samples from patients without a CMPD. Although AS-PCR and PCR-RFLP typically yielded concordant results, the efficiency of DNA amplification in archival material differed significantly between these two methods. Finally, dilution studies demonstrated that both methods may artifactually yield a heterozygous pattern in a homozygous specimen contaminated with different percentages of normal DNA.
Conclusions: *JAK2* (V617F) mutations may be detected in both fresh and archival material using either of the two PCR-based methods evaluated. The proportion of non-CML CMPD patients with a detectable *JAK2* (V617F) mutation in this series is in general agreement with that observed in other studies. Although both methods typically yielded concordant results, they differed with respect to efficiency of DNA amplification in archival material. In addition, both methods may artifactually yield a heterozygous pattern when homozygous DNA is contaminated with different percentages of normal DNA, suggesting that clinical reporting of absence or presence of the mutation may be preferable to assignment of heterozygous or homozygous status on the basis of these assays. Finally, the detection of a *JAK2* (V617F) mutation in specimens with equivocal pathologic findings may support a definitive diagnosis of a CMPD.

1521 FISH Analysis of Immunoglobulin Heavy Chain Translocations in Plasma Cell Myeloma Using Intact Paraffin Sections and CD138 Immunofluorescence
JR Cook, J Pettay, M Hartke, RR Tubbs. Cleveland Clinic Foundation, Cleveland, OH.
Background: Approximately 50% of plasma cell myeloma cases contain translocations involving the immunoglobulin heavy chain (*IGH*) locus, some of which are associated

with distinct clinicopathologic features that may be useful in diagnosis and prognostic assessment of these neoplasms. However, metaphase cytogenetic studies are often unsuccessful due to the low proliferative rate of plasma cells in culture. Standard FISH assays are complicated by the fact that the plasma cells may represent only a minor component of the bone marrow cellularity. To overcome these obstacles, we have developed a novel interphase FISH assay using intact paraffin sections of bone marrow clot preparations with simultaneous CD138 immunofluorescence.
Design: 20 cases of plasma cell myeloma, with plasma cells ranging from 6-88% of the cellularity, were analyzed using 5μm sections of paraffin embedded, formalin fixed bone marrow clot preparations. To preserve CD138 signal during subsequent deparaffinization and protease K treatment, staining was performed using a tyramine signal amplification (TSA) system with an Alexifluor label. All cases were analyzed using a dual color, break-apart probe for *IGH* and dual color, dual fusion probes specific for t(11;14)(q13;q32) and t(4;14)(p16;q32). 100-200 nuclei of CD138 positive cells were counted.
Results: TSA-mediated deposition of the Alexifluor label in CD138 positive plasma cells was unaffected by protease digestion. Using the break-apart probe, 8 cases were found to contain *IGH* translocations, shown by dual fusion probes to be 5 cases with t(11;14)(q13;q32) and 3 cases with t(4;14)(p16;q32). All cases positive with one of the dual fusion probes were also positive by the break-apart method. In translocation positive cases, abnormalities were identified in a high percentage of cells counted (62-91%, median 78%), even when plasma cells were few in number. Conventional cytogenetic analysis identified abnormal karyotypes in 8 cases, but did not identify any of the *IGH* translocations.
Conclusions: Simultaneous interphase FISH and immunofluorescence using TSA allows for selective genotyping of specific cell types in intact paraffin sections. In plasma cell myeloma, this technique allows for identification of abnormalities with diagnostic and prognostic implications that may not be detected by metaphase cytogenetics. A break-apart probe for *IGH* translocations can be used to efficiently screen for these abnormalities in plasma cell myeloma.

1522 Tissue Fixation in Surgical Pathology for Proteome Analysis and Protein/DNA Preservation
DJ Dabbs, T El-Hefnawy, DE Malehorn, R Elbakri, WL Bigbee. Magee-Womens Hospital of UPMC, Pittsburgh, PA; University of Pittsburgh Cancer Institute, Pittsburgh, PA.
Background: Formalin-fixed paraffin embedded tissue is ideal for tissue morphology and a variety of ancillary tests in surgical pathology, but proteins and DNA are rendered inactive for advanced molecular studies and proteomics. In this study we compare the qualities of protein and DNA between frozen tissue and tissues fixed in a formalin-free Universal Molecular Fixative (MFIX) and embedded in paraffin.
Design: Total proteins were extracted from 16 frozen breast tissue samples (8 normal and 8 malignant) and from paired, deparaffinized MFIX processed tissue sections using 8M urea, 4% CHAPS, 40 mM Tris-Cl and 100 mM DTT buffer. Integrity of the proteins from MFIX tissues was verified by resolving 5 mg of each protein sample on SDS-polyacrylamide gels. We further evaluated the usefulness of the recovered proteins to distinguish between malignant and normal breast tissues using protein profiling on SELDI-TOF mass spectrometry. Approximately 10 mg of total proteins were allowed to bind to individual spots on IMAC3-Cu® protein array chips using 10 h incubation. The free proteins were washed and profiling analysis of the extracted proteins was performed on the Ciphergen PBS-IIC ProteinChip® Array Reader. DNA was extracted using DNAzol® lysis buffer and quantitated using spectrophotometrical analysis of light absorption at l260/280.
Results: Silver staining of the prominent protein bands demonstrated a qualitatively similar protein pattern between frozen and MFIX tissue sections. The protein quantity was comparable between M-fixed tissues and frozen tissue sections. The SELDI-TOF mass spectrometry analysis of MFIX tumor extracts showed unique protein signals (e.g. 3158 Da classifier) from baseline subtracted & normalized spectra that generated 100% tree separation between M-fix normal and tumor breast tissues. The total DNA recovered from MFIX processed deparaffinized tissue sections was quantitatively comparable to those of paired frozen tissue samples. DNA from both processing methods was amplifiable as tested by PCR analysis of the 18S gene.
Conclusions: (1) While demonstrating acceptable tissue morphology, MFIX paraffin embedded tissues also provide preservation of protein and DNA molecular signatures and can be a very useful tool for both proteomics and nucleic acid-related research protocols. (2) MFIX tissues is an economic method of archiving paraffin blocks providing a database of tissues previously unavailable for the study of disease.

1523 Impact of Pre-Analytic Factors on Stability of Phosphoproteins: Implications for Clinical / Preclinical Biomarker Studies
JD Deeds, MF Loda, R Meyer, Y Shim, JM Mosquera-Buitrago, RE Mosher. Novartis Institute for BioMedical Research, Cambridge, MA; Brigham and Women's Hospital, Boston, MA.
Background: Protein phosphorylation is a ubiquitous and highly specific intracellular signaling mechanism in tumor cell biology. IHC for phosphoproteins has great potential for evaluation of predictive and functional biomarkers. Samples collected reterospectively for epidemiologic surveys or prospectively during clinical trials may not be processed consistently. Prior to conducting IHC studies with such material, it is critical to assess the impact of preanalytic variables on the markers of interest. We examined the impact of tissue ischemic times to determine the impact on phosphoprotein expression patterns.
Design: The effect of delayed fixation on the phosphostatus of a number of important signaling proteins relevant to cancer biology (including pS6, pSTAT3,pMEK) was evaluated. A375 subcutaneous melanoma xenografts were rapidly excised, sliced into five pieces approximately 5mm thick and placed into room temperature PBS. Samples

were removed from PBS and placed into NBF after 0, 5, 15, 30 and 60 minutes. All samples were fixed in NBF for 2 hours at RT and then processed to paraffin using conventional methods. Samples from four animals were also snap frozen at each timepoint for examination by Western Blot. Freshly cut slides were stained using the Ventana Discovery. Different protocols, including varying cell conditioning methods were tried. Slides were scanned by Aperio ScanScope and staining intensity/distribution was assessed by automated imaging routines developed with ImageJ and Aperio ImageScope. Independent manual evaluation by pathologists (REM, MFL, JMB) confirmed the results of these analyses and provided additional synoptic information. **Results:** The marker expression intensity varied as the same xenograft tissues were examined over the series of time points. Some protein phosphorylation (pSTAT3) was apparently decreased over time as tissues were held in PBS; some protein phosphorylation (pMEK) showed an apparent increase as time in PBS increased. Western blot results confirmed observations made by IHC.
Conclusions: For some phosphoprotein markers, effects of prefixation ischemic times may significantly impact their utility as clinical biomarkers for patient stratification and pharmacodynamics unless the collection and handling of samples is highly controlled. Some of these markers may be able to be used as QC measures of sample collection adequacy.

1524 Diagnostic Fluorescence Microscopy Improved by Light Emitting Diodes (LED) Technology
AP Dei Tos, M Angelini, MC Giangarè, N Baraldo, G Mazzini. Hospital of Treviso, Treviso, Italy; Fraen Corporation, Milan, Italy; IGM-CNR, University of Pavia, Pavia, Italy.
Background: Since many decades, fluorescence microscopy has proved very useful in both diagnostic pathology and research. Immunofluorescence still represents a powerful tool and, fluorescence "in situ" hybridization (FISH), is increasingly gaining popularity. Several fluorescent molecules, like Fluoresceine-Iso-Tio-Cianate (FITC), are efficiently excited by blue light sources such as Argon ion laser line at 488nm; however, they tend to be suboptimally excited by the blue band (450-490nm) delivered by the mercury arc lamp of standard fluorescence microscopes. Moreover, mercury lamp emission often shows low efficiency with fluorochromes excited in the red spectral region. In consideration of the recent advances of light emitting diodes (LEDs) technology, a joint venture between research institutions and industry is currently dealing with advanced solid state excitation devices aimed to replace arc lamp excitation sources for both fluorescence microscopy and flow cytometry.
Design: Different prototypes of excitation modules, fitting most commercially available microscopes and operated by both epi-illumination and transmitted light, were constructed. Instrumental and "visual" comparisons between LEDs and lamp excitations were carried out. Instrumental measurements were performed with a power meter located either under the microscope objectives or mounted on a modified Abbe condenser. Visual comparison was performed on a variety of human tissue samples stained with DAPI, anti actin and anti tubulin antibodies labeled with several fluorochromes.
Results: The excitation performance of 3Watts LEDs and 100Watts mercury arc lamp were comparable. A significant increase of signal-to-noise ratio was achieved particularly with an original "transmitted excitation" set up by mean of both 2Watts UV (365nm) and 3Watts Blue (485nm) LEDs, delivering up to some hundreds milliWatts within narrow spectral bands (15nm). FITC and FITC-like fluorochromes labeling observation appeared consistently improved by blue LED excitation, whereas the optical power emitted by a mercury arc lamps in the same spectral region was lower. **Conclusions: 1.** First successful application of LEDs technology to fluorescence microscopy represents a major technological advance, allowing significant improvement of both image quality and system efficiency. **2.** Indefinite LEDs' life-expectance associated with lower costs may allow broader use of fluorescence-based investigative techniques.

1525 Detection of Monoclonal Immunoglobulin Heavy Chain Gene Rearrangements in Diffuse Large B-Cell Lymphomas Using a Subset of the BIOMED-2 Primers
LJ Dobbs, L Earls, A Ahsanuddin, K Hewan-Lowe. Brody School of Medicine at East Carolina University, Greenville, NC.
Background: The diagnosis of B-cell malignancies often involves the use of molecular testing to establish the monoclonal nature of the suspected lymphoid neoplasm. One of the most commonly used methods is PCR based testing using degenerate primers to the framework region 3 (FRIII) and joining region (Jh) of the immunoglobulin heavy chain (IgH) gene. However, using these primers only around 70% of all B-cell lymphomas can be shown to be monoclonal. Even fewer (50%) of diffuse large B-cell lymphomas (DLBL) can be shown to be monoclonal using these primers. Recently, the BIOMED-2 primers were reported to improve the sensitivity of PCR based testing for IgH gene rearrangements. We tested a subset of the BIOMED-2 primers for the ability to detect monoclonal IgH gene rearrangements in a selected group of lymphomas (DLBL).
Design: We selected 54 cases of DLBL that had been previously tested for a monoclonal IgH gene rearrangement using PCR and the FRIII/Jh primer pairs. We then used PCR and a subset of the BIOMED-2 primers that encompass the heavy chain gene families and tested these same cases for the presence of a monoclonal IgH gene rearrangement. These results were then compared with the results obtained using the FRIII/Jh primers, serving as a direct comparison of the clinical sensitivity of the two methods.
Results: When the FRIII/Jh primers were used, monoclonal IgH gene rearrangements were detected in 26/54 cases (sensitivity = 48%) of DLBL. In contrast, when the heavy chain subset of the BIOMED-2 primers were used, the detection rate improved significantly to 35/54 (sensitivity = 65%). Equivocal results were obtained in 6/54 cases using the FRIII/Jh primers, while only 2/54 gave equivocal results using the BIOMED-2 primers.

Conclusions: When compared with the conventional FRIII/Jh primers, the BIOMED-2 primers significantly improved the ability to detect monoclonal IgH gene rearrangements using PCR in cases of DLBL. However, the multiplex reaction is much more cumbersome to setup, and requires at least two polyacrylamide gels if conventional polyacrylamide gel electrophoresis is used. In addition, the BIOMED-2 primers are less robust than the FRIII/Jh primers, likely secondary to the multiplex PCR reaction. Therefore, although the BIOMED-2 primers are more sensitive than the conventional FRIII/Jh primers, the decision to replace the conventional FRIII/Jh primers with the BIOMED-2 primers should take these technical differences into consideration.

1526 Real Time PCR Detection of a JAK2 Mutation in Polycythemia Vera Patients
SD Dufresne, DR Belloni, SL Ketchum, MK Cornell, A Kominski, S Chaffee, P Ely, JM Hill, CJ Cornell, GJ Tsongalis. Dartmouth-Hitchcock Medical Center, Lebanon, NH.
Background: The diagnosis of Polycythemia Vera (PV) is based on a combination of clinical criteria, laboratory tests and bone marrow biopsy findings. However, the diagnosis can be difficult to make since the findings are variable at different stages of the disease and some cases may be difficult to separate from secondary causes of polycythemia. Recently, a mutation in the *Janus Kinase 2* (*JAK2*) gene resulting in a valine to phenylalanine substitution at position 617 has been identified that is present in 65-97% of patients with PV. Although this mutation may also be found in 23-57% of patients with essential thrombocythemia (ET) or myelofibrosis, it is consistently absent in normal controls and patients with secondary polycythemia. Identification of this mutation could be helpful in establishing a diagnosis of PV. PCR amplification of the mutated segment followed by sequencing is the method generally used to identify this mutation. However, this is an expensive and time consuming process. Our goal was to develop a rapid and reliable means of identifying this JAK2 mutation using a TaqMan SNP genotyping assay.
Design: DNA was isolated from either peripheral blood or bone marrow aspirates from six patients with PV, seven patients with either ET or myelofibrosis, and sixteen patients without these disorders including nine patients with secondary polycythemia. Sequence flanking the region of the *JAK2* gene containing the $JAK2^{V617P}$ mutation was submitted to Applied Biosystems. They provided a SNP genotyping Assay-by-Design, which was used with ABI 2X Fast Universal Master Mix. A 10 μl reaction was run using the default fast cycling conditions on the ABI 7500 Fast Real-Time PCR System. A post-amplification plate read was done and the data analyzed using the SDS software supplied with the instrument. Using the ABI Fast System, JAK2 analysis was completed within 1 hour.
Results: The JAK2 mutation was identified in all six PV patients using the TaqMan SNP assay. The mutation was also present in five of the seven patients with either ET or myelofibrosis. In contrast, the mutation was absent in all 16 patients without these myeoloproliferative diseases, including nine patients with secondary polycythemia.
Conclusions: The TaqMan SNP genotyping assay provides a rapid and specific means of identifying the JAK2 mutation in patients with PV or other myeloproliferative disorders. This method can be a useful aid in differentiating patients with PV from those with secondary polycythemia.

1527 Impact of Internet Based Resources on Resident Teaching and Educational Conferences: Experience at a University Affiliated Hospital Network Comprising Academic and Community Based Pathology Practices
JL Fine, Y Yagi, AV Parwani, MJ Becich, JR Gilbertson. University of Pittsburgh Medical Center, Pittsburgh, PA.
Background: Our geographically distributed hospital network comprises 19 hospitals, four of which are academic centers with subspecialty pathology sign-out. This milieu presents challenges to department wide resident education and academic conferencing. The Internet and other information technologies have been utilized to address these challenges, resulting in a large resource of on-line teaching cases, archived conferences, and annotated whole slide image teaching sets. These are collected primarily in the departmental web site (http://path.upmc.edu) as well as the departmental telepathology web site (http://telepathology.upmc.edu).
Design: The educational and academic mission of the distributed department is supported by three web-based systems: 1) a collection of multimedia teaching cases that are authored by residents and faculty (http://path.upmc.edu/cases.html); 2) daily internet broadcast and subsequent archival of the main academic conferences (http://teleconference.upmc.edu/pathconf/); and 3) subspecialty-based teaching collections of whole slide images created from glass slides. Scanning and annotation of the teaching collections is ongoing and will represent a substantial investment of departmental resources when complete.
Results: These resources have been accepted by residents, faculty, and departmental leadership. Currently 439 teaching cases and 639 archived departmental conferences are online with 60 to 100 unique users in a typical month, including 4,193 images. More than 2,750 whole slide images have been created, including a general pathology collection and four subspecialty collections (dermatopathology, bone and soft tissue, neuropathology, and genitourinary). The process of annotation is ongoing.
Conclusions: These internet-based pathology informatics resources have enriched our pathology educational and clinical resources. These resources have facilitated pathology education in a multi-hospital, partially subspecialty sign-out environment, and are readily available to all residents and faculty at our health system. These substantial digital media resources are widely utilized and represent a significant investment by a pathology department in order to facilitate pathology education and serve as a model for other institutes as they build their digital archives.

1528 High-Quality Preservation of RNA and Morphology in Paraffin
AH Fischer, Z Mou, BA Woda. University of Massachusetts, Worcester, MA.
Background: High quality preservation RNA (e.g., the large 28 and 18S ribosomal RNAs) has not been achieved in paraffin embedded tissue. We systematically studied the paraffin embedding process to determine at which point(s) RNA is degraded. The findings were adapted to achieve simultaneous preservation of morphology and RNA in paraffin embedded tissue.
Design: HeLa or DU-145 tissue culture cells were scraped from log-phase culture plates. The stability of their RNA in various storage media, isopropyl alcohol (as a dehydrating agent), xylene, and paraffin was then studied. RNA stability was expressed as the ratio of 28 to 18s ribosomal RNA, as measured by densitometry after isolation and electrophoresis of total RNA through a 1% agarose denaturing gel.
Results: Using a ratio of 28/18S rRNA of more than 1.8 as a definition of preserved RNA, RNA was preserved in RNAlater™ for weeks, but cellular-level morphology was very poor. The poor nuclear morphology could not be reversed by washing with balanced saline or dilute alcohol solutions. RNA was stable for >5 minutes but <1 hour in 70% aqueous isopropyl alcohol at room temperature (RT). RNA was stable in Cytolyte™ at RT for more >1 hour, but < 18 hours. RNA was stable in Preservcyt™ at RT for >18 hours but <1 week. RNA was stable in 100% isopropyl alcohol >18 hours at RT. After being brought quickly through 100% isopropyl alcohol, RNA was stable in xylene at RT for >18 hours. Using a new "rapid cell block" embedding apparatus (see separate abstract), tissue fragments less than 1 mm can be completely dehydrated in less than about 3 minutes. Using the rapid cell block technique with alcohol-based fixation and dehydration, RNA remains well preserved in paraffin for >1 week with excellent simultaneous preservation of morphology. In general, morphology did not seem to be affected by whether or not RNA was preserved.
Conclusions: The susceptibility of RNA to degradation is during the dehydration step. If dehydration can be performed quickly, e.g., with the "rapid cell block technique" using relatively small pieces of tissue about 1 mm in diameter, morphology and RNA can be simultaneously preserved. The technique should permit a wider range of analysis of RNA in pathologic processes (e.g., examination of 3' non-coding regions of genes, or analysis of micro-RNA's) when only small numbers of cells (e.g., microdissected cells) are available.

1529 Multispectral Imaging of Cellular Targets Using Semiconductor Quantum Dots
T Fountaine, S Wincovitch, D Geho, S Garfield, S Pittaluga. NCI, Bethesda, MD; CCR Confocal Microscopy Core Facility, NCI, Bethesda, MD.
Background: Organic fluorophores have been extensively used in immunohistochemical analyses using frozen and/or formalin-fixed paraffin embedded tissue sections (FFPE). A novel nanotechnology, the quantum dot (an inorganic fluorophobe), offers a versatile alternative reporter system due to its intrinsic characteristics (stability, resistance to photobleaching, wide excitation range and narrow emission spectra).
Design: The aim of this study was to be able to detect multiple targets using streptavidin-conjugated quantum dots (SA-QDs) on FFPE tissue sections. Biotinylated secondary antibodies were applied followed by individual SA-QDs of different wavelengths (525nm, 565nm, 585nm, 605nm, 655nm, 705nm). Multiple targets were identified by sequential staining rounds. Images were acquired using a Zeiss LSM 510 NLO confocal system and the 488nm line from a 30mW Argon laser. The assorted SA-QDs emissions were collected with a Zeiss meta detector.
Results: To establish staining and image acquisition conditions, we chose well known primary antibodies that are routinely used in the diagnosis of lymphoid malignancies. CD20 and Ki-67 exhibited membranous and nuclear staining, respectively, with the expected tissue distribution. The emission profiles of SA-QDs were verified using a novel technology for confocal microscopy known as emission fingerprinting; x-y scans were made across a series of wavelengths generating a lambda stack. A typical emission fingerprint was generated for each SA-QD using CD20 and Ki-67. By optimizing signal intensity, primary antibody and type of target we could detect up to 5 signals plus DAPI in FFPE sections.
Conclusions: Quantum dot technology was found to be a useful alternative method to traditional organic fluorophores. The multispectral staining exhibited high specificity, low background and high emission intensity. The stained sections could be re-analyzed after a prolonged period of time, and no photobleaching was noted. The images were captured using a laser point scanning confocal microscope and a Meta detector consisting of a PMT array. The fact that multiple Qdots can be excited with a single laser excitation line, 488 nm for these studies, provides the advantage of using a less expensive excitation source for detection of multiple emissions. The relatively narrow emission peaks of SA-QDs allowed the use of multiple (3 to 5) antibodies on a single tissue section.

1530 Automated Analysis of Chromatically Stained Tissue Sections by Three Laser (RBG) Scanning Cytometry
WR Geddie, E Luther. University of Toronto, Toronto, ON, Canada; CompuCyte Corporation, Cambridge, MA.
Background: Visual assessment of tissues stained with several chromatic dyes or those stained with both chromatic and fluorescent dyes is complex, and instrumentation and software have not existed for automated analysis. The iColor®, a unique imaging cytometer with red, green and blue lasers is capable of measuring RBG color absorbance in separate channels along with multichannel fluorescence, and providing high resolution images. In order to construct a paradigm for automated cytometric analysis of tissue microarrays (TMA(s)) with this instrument we studied tissue sections stained with a variety of chromatic dyes.
Design: IPOX stains of different tissues developed with DAB and counterstained with hematoxylin or nuclear fast red; pancreas dually stained with conventional DAB,

NiDAB and hematoxylin; and renal cell carcinoma dually stained with DAB, Alkaline Phosphatase (Fast Red) and hematoxylin were evaluated. From a low resolution tissue map areas of interest were selected for simultaneous high resolution scanning with three lasers and capture of RBG absorbance data and multispectral fluorescence. Image algebra allowed compensation for the spectral overlap of the dyes. Constituent expression levels were calculated for nuclear or membrane antigens by either cellular quantification or random sampling based techniques.
Results: Two laser absorbance measurements were sufficient for separating hematoxylin or Fast Red from DAB absorbance. Three lasers were employed to completely separate the constituents in the dual stained renal carcinoma slide, allowing separate images of specific staining of different compartments. Because fast red is fluorescent, independent verification of the absorbance correction algorithms was possible for this chromogen. Conventional DAB and NiDAB absorbance were partially separated using the compensation techniques, and regions of selective staining were quantified. With the three laser system, near real color imaging was achieved.
Conclusions: This instrumentation creates a "virtual slide" containing multichannel absorbance and fluorescence data that can be used for automated cytometric analysis of tissues and TMA's stained by a double chromagen immunlabelling method, and simultaneous assessment of fluorescent signals. The high resolution images constructed from the data allow precise selection of areas of interest. The ability to compensate for spectral overlap ensures that pertinent signals from different cellular compartments can be quantitated.

1531 Reproducibility of 2D-DIGE for Determining Differences in Protein Expression Levels in Complex, Low-Abundance Samples: Implications for Biomarker Discovery
O Greengauz-Roberts, R Podulsky, H Stoppler, D Ferris, JR Lee, WS Dynan. Medical College of Georgia, Augusta, GA; Veterans Affairs Medical Center, Augusta, GA.
Background: The combination of laser capture microdissection (LCM) and two dimensional-difference gel electrophoresis (2D-DIGE), with saturation dye labeling enables proteomic profiling of pure cell populations containing as little as 1 microgram total protein. Herein, we investigate reproducibility of the LCM/2D-DIGE technology based on repeated sampling of the same biological specimens.
Design: Specimens included normal human cervical epithelium, cervical squamous cell carcinoma, poorly differentiated ovarian carcinoma, and ovarian cystadenoma. For comparison, analysis was also performed using bulk protein from an animal liver specimen. Each specimen was sampled three times by LCM and analyzed by 2D-DIGE. We used an indirect comparison design, where an invariant internal standard was present in every gel within a group. Gels within each group were matched, and for each protein spot, we determined the mean and standard deviation of abundance relative to the internal standard, and from these the coefficient of variation (CV).
Results: Median CVs ranged from 9% to 24%, with normal human epithelial tissue exhibiting the greatest variability, tumor specimens intermediate variability, and animal liver extracts the least. Significant differences (p<0.05) were seen for 39 protein spots in the human cervical epithelium: cervical cancer pair and for 29 spots in the human ovarian cystadenoma: carcinoma pair. A dye-reversal experiment determined that dye bias is not a limiting factor.
Conclusions: This study provides an estimate of the magnitude of technical variation encountered in the overall pathway of protein analysis by LCM/2D-DIGE. Based on the observed reproducibility, studies with 10-15 patient specimens per group should have adequate power for an initial phase of biomarker discovery.

1532 Chronic Lymphocytic Leukemia with Intermediate Rates of VH Mutation Encompass Both Pre-Germinal and Post-Germinal Subsets
C Hannah, R Luthra, JL Jorgensen, D Jones. University of Texas MD Anderson Cancer Center, Houston, TX.
Background: CLL is divided into pre- and post-germinal center (GC) subsets based on degree of changes in the immunoglobulin heavy chain variable region (VH) of the tumor clone arising through somatic hypermutation (SHM). The unmutated/pre-germinal center subset is thought to have a more aggressive clinical course. Surrogate markers of the unmutated subset, CD38 and ZAP70 expression, are known. Recent studies question if the mutation rate is due partly to overexpression of the SHM machinery or if it is a reflection of histogenesis. Therefore, we analyzed the patterns of mutation by antigen selection (AS) bias and VH usage in CLL cases with intermediate rates of VH mutation (SH-mid, 1.5-4% of total in VH coding region) and compared them to ZAP70 and CD38 expression and their clinical features.
Design: SHM was determined by cDNA isolated from peripheral blood (PB) or bone marrow (BM) of CLL samples and multiplex PCR (VH1-6, CH and/or JH primers) followed by DNA sequencing of the dominant clone VH region. The percent deviation from germline was determined by comparison with IMGT IGH database. Replacement versus silent mutations in CDR and framework regions was used as evidence of AS process (true post-GC tumor). Probability of AS was derived by the method of Lossos et al (www-stat.stanford.edu/immunoglobulin). Results were compared with assessment of ZAP70 by paraffin section immunohistochemistry on BM cores and CD38 expression by flow cytometry on parallel BM or PB. Usage of VH was compard in a group of 527 CLL cases.
Results: We assessed for AS in 52 cases of B-CLL of SH-mid and compared them to 22 heavily mutated cases (SH-high, >4% divergence). Among 52 cases of SH-mid CLL, 22 (42%) were predicted to have bias in mutation indicative of antigen selection versus 18 of 22 (82%) SH-high cases. ZAP70 was expressed in 46% (16/35) of SH-mid cases versus only 2 of 22 (9%) SH-high cases. CD38 was expressed in >20% of tumor cells in 12 of 51 (24%) SH-mid CLL versus only 1 of 22 (5%) SH-high cases. Cases utilizing VH3-21 were found more frequently in SH-low (11/258, 4.3%) and SH-mid (7/86, 8.2%) than in SH-high cases (2/192, 1%). A strong inverse correlation between mutation rate and Rai score at time of presentation was found in all cases.

Conclusions: Many cases with intermediate rates of VH sequence divergence appear similar to unmutated cases (ZAP70 and CD38 expression, low AS bias). Determination of anitgen selection probability in these cases will help in categorization as pre-GC or post-GC subtypes.

1533 Use of Whole Slide Imaging for Primary Diagnosis in Surgical Pathology: An Intrainstitutional Validation Study

J Ho, D Jukic, A Parwani, L Anthony, J Gilbertson. University of Pittsburgh Medical Center, Pittsburgh, PA; University of Pittsburgh, Pittsburgh, PA.

Background: Whole slide images (WSI) have the potential to streamline workflows, increase productivity, and may provide additional capabilities such as computer aided diagnosis. However, only a few studies describe a comparison of WSI with microscopic examination in clinical activities. We evaluate the use of WSI for anatomical pathology (AP) signout.

Design: Our objective was to simulate a routine pathology signout experience with the exception that glass slides were replaced by WSI. 3 pathologists each signed out the same 25 full genitourinary pathology and dermatopathology cases within a 1 month period. Pathologists received their worklists, ordered recuts and special stains, and created final reports through the AP information system. At the conclusion of the study, the diagnostic reports of the individual study pathologists were compared and a consensus report was created. The consensus reports were then compared to the original reports rendered from glass slides. Following this, study pathologists were debriefed and surveyed by the evaluation team.

Results: A total of 535 WSI were examined. Each pathologist evaluated an average of 178 WSI. Cases ranged in size from 3 to 24 initial H&E stained slides, and included skin and prostate biopsies, vasectomies, a radical nephrectomy, and a transurethral prostate resection, among others. Discrepancies between study pathologists were categorized into 4 types. 17 cases showed complete agreement between study pathologists. Of the 8 discordant cases, 4 were due to non-image related issues such as inexperience and reporting styles. Four cases were partially associated with image quality issues that were largely focus-related. In all cases the WSI-based consensus agreed with the original final report. Pathologists were mostly concerned with workflow inefficiencies. They noted that the WSI interface was not integrated with the AP system, and was also not as intuitive as the microscope.

Conclusions: WSI retain enough visual information for pathologists to reliably deliver final reports that are equal to microscopic methods. While visual information was sufficient, cumbersome WSI presentation significantly increased the required effort for a pathologist to evaluate a specimen.

1534 Optimizing DNA Amplification from Ancient Human Remains

K Johnson, M Allison, M Torbenson. Johns Hopkins University School of Medicine, Baltimore, MD; Virginia Commonwealth University, Richmond, VA.

Background: DNA from ancient sources (aDNA) such as mummies or old paraffin blocks holds great promise for understanding human disease. aDNA can potentially be queried for specific gene mutations as well as for infectious diseases. However, limits to aDNA include the low amounts of DNA in mummified tissues, extensive DNA fragmentation (typically 250bp average size), and DNA damage. To aid in the study of aDNA, enzyme mixtures that include DNA repair proteins may be helpful. Also, non-specific amplification steps, such as random primer PCR or random strand displacement amplification (RSDA), may be useful in increasing the total amount of template DNA prior to gene specific PCR.

Design: Using skeletal calf muscle from a naturally mummified 21-year-old male body (Chiribaya culture, Peru, 1000 BP), we amplified the human beta-catenin gene in triplicate under the following conditions: (1) single round traditional PCR; (2) single round PCR with an enzyme mixture designed to repair damaged DNA (Restorase DNA Polymerase, Sigma-Aldrich); (3) random primer PCR followed by beta catenin PCR, (4) random primer PCR followed by RSDA (GenomiPhi, Amersham) and then beta-catenin PCR.

Results: DNA concentrations were 50 µg/ml following DNA extraction, 75 µg/ml following random primer amplification, and 4500 µg/ml after random primer PCR plus RSDA. The average DNA fragment size was not determined after DNA extraction and after random primer PCR due to low DNA concentrations, but following RSDA, the average size DNA fragment was 5 kb based on agarose gel electrophoresis. For PCR studies, numerous water controls were included at all steps and all were negative. Beta catenin DNA was amplifiable under the following conditions: (1) 0/3 replicates with traditional PCR; (2) 3/3 replicates with Restorase PCR; (3) 1/3 replicates with random primer PCR followed by traditional PCR; and (4) 3/3 replicates after random PCR and RSDA.

Conclusions: Multiple strategies can enhance DNA analysis when working with aDNA. Restorase enzyme mixtures appear to be particularly useful when PCR is performed using extracted, non-amplified DNA as template. Random primer PCR and random strand displacement amplification, either alone or in combination, can increase the total amount of available DNA template prior to gene specific amplification. Random strand displacement amplification may also preferentially amplify larger DNA fragments.

1535 Application of Array CGH on Archival Formalin Fixed Paraffin Embedded Tissues

NA Johnson, R Hamoudi, K Ichimura, L Liu, D Pearson, P Collins, M-Q Du. University of Cambridge, Cambridge, United Kingdom.

Background: Array-based comparative genomic hybridisation (aCGH) is increasingly used for investigation of chromosomal gains and losses in diseases, particularly cancers. It is a robust and versatile technology with potential in both research and clinical investigations. Currently, aCGH is performed primarily using high molecular DNA extracted from fresh frozen tissues or cells. It remains to be established whether aCGH can be reliably applied to archival formalin-fixed paraffin-embedded (FFPE) tissues and further applied to small numbers of cells microdissected from a defined histological lesion.

Design: DNA samples purified from nine FFPE glioblastoma xenograft tissues were subjected to aCGH analysis using a well-established in-house human 1MB genomic array. The quality of array data from FFPE was compared to that of the matching frozen tissue in each case and then correlated with the quality of DNA, which was assessed by amplification of variable sized gene fragments. The sensitivity of aCGH to detect genomic gains and losses was examined using serially diluted tumour DNA samples. The minimum number of cells and amount of DNA from FFPE tissues required for successful aCGH were also investigated following whole genome amplification (WGA).

Results: All 9 frozen xenograft tumours yielded high quality aCGH data showing characteristic chromosomal imbalances of glioblastoma. By comparison with the aCGH profile of frozen tissues, 3 of the 9 FFPE xenograft tumours showed high quality reproducible aCGH data and all 3 FFPE samples displayed strongly amplified DNA fragments ≥400 bp in size. In contrast, the remaining 6 FFPE that gave poor aCGH results failed to amplify fragments ≥400 bp in size. Formalin fixation up to 96 hours and storage of FFPE tissue up to 15 years did not appear to have a major effect on aCGH analysis, while presence of necrosis dramatically increased the background. In addition, highly sensitive detection required tumour cells above 70%. As little as 10ng DNA from frozen or FFPE tissue could be readily used for aCGH analysis following WGA and as few as 2000 cells microdissected from sections of FFPE tissues could be successfully used for aCGH when WGA was incorporated.

Conclusions: Genomic DNA from archival tissue is suitable for aCGH analysis if the DNA quality supports routine PCR amplification of DNA fragments ≥400 bp in size. Combination of microdissection and WGA allows aCGH analysis of a small number of cells microdissected from a defined histological lesion, such as carcinoma *in situ*.

1536 Sequential Scrubbing Technique for Combinations of Molecular Abnormalities Identify Low Stage, Non-Small Cell Carcinoma of the Lung That Do Not Need Chemotherapy

DL Jones, JF Silverman, YL Liu, RS Saad, R Keenan, CA Smith, SE Shackney. Allegheny General Hospital, Pittsburgh, PA; Laboratory of Cancer Cell Biology and Genetics, Pittsburgh, PA.

Background: The outcome of low stage non-small cell lung cancer (NSCLC) patients varies (Stage I NSCLC: 60% 5 yr. survival; Stage II: 40% 5 yr. survival). We evaluated a novel technique of data scrubbing of molecular abnormalities to separate the disease-free survival of two groups, and cull out the unfavorable group needing chemotherapy.

Design: Laser Scanning Cytometry (LSC) was performed on fixed single cell suspensions from 48 primary NSCLC patients with low stage NSCLC having a median follow-up of at least six months. Histologic types were 24 adenocarcinomas, 19 squamous cell carcinomas, 4 large cell carcinomas, 1 adenosquamous cell carcinoma. LSC analyzed four quantitative correlated fluorescence measurements per cell consisting of DNA content, Her2/neu, EGF receptor and VEGF on each of several hundred to several thousand (K) cells per tumor sample. Repetitive sequential analysis were performed with scrubbing #1 identifying cells with EGFR > 30K molecules (mol.)/cell, Her2/neu > 100K mol./cells, and aneuploidy > 3% in the same cells. Scrubbing #2 identified cells with Her2/neu > 1000K mol./cell, VEGF > 1000K mol./cell and aneuploidy > 3% in same cells. Scrubbing #3 identified cells negative for EGFR and VEGF and aneuploidy.

Results: There was 13 recurrences (R) in 48 patients. Scrubbing #1 identified 4 R and 2 NR. Scrubbing #2 identified 3 additional R and 4 NR. Scrubbing #3 identified 3 additional R and 1 NR. Therefore, using repetitive data analysis, 10 of the original 13 R were identified using the three different combinations of sequential analysis. In Stage IA, there were 4 R/21 patients; IB, 7 R/18; Stage IIA, NR in 1 patient and Stage IIB, 2 R/8.

Conclusions: By using a repetitive scrubbing technique for molecular analysis, 10 of the original 13 R were identified in low stage NSCLC. The net effect divided patients populations into two subsets, one of which culled out cases that recurred (10/23) (43%) in comparison with the original population in which 13/48 (27%) recurred and separate them from the more favorable group having only 3/25 (12%) R. This analytical technique can be extended with the therapeutic goal of having a false negative rate for the favorable group reduced <5% to better identifying patients in low stage NSCLC that need chemotherapy from those better left untreated.

1537 Developing Techniques in High-Throughput Telomere Analysis for the Study of Prostatic Carcinogenesis

AM Joshua, C Mei, I Braude, T Collins, B Vukovic, JR Srigley, AJ Evans, JA Squire. Ontario Cancer Institute - Princess Margaret Hospital, Toronto, ON, Canada; Le Chesnay Cedex, France; The Credit Valley Hospital, Mississauga, ON, Canada; University Health Network, Toronto, ON, Canada.

Background: There is increasing interest in the prognostic value and role of telomeres in the pathogenesis of a variety of carcinomas. Advances in fluorescence microscopy and peptide nucleic acid probes have facilitated the analysis of telomere length on paraffin-embedded sections of clinical biopsies by fluorescence in situ hybridization (FISH). To date, quantification and thresholding of telomeres on these sections have been user-dependent. We present an Otsu thresholding alogorithm incorporated into an "Image J" macro and a Perl-based script to provide automated analysis of the telomere fluorescence signal and normalized output.

Design: Twelve-bit greyscale images are produced using a Leica epiflourescence microscope with a Hammatasu camera (ORCA ER-17). The existing Image J macro for Otsu thresholding was rewritten and combined with macro scripts for automated analysis. Appropriate nuclei are identified on the DAPI image and the corresponding fluorescent image is run through the rolling ball background subtraction algorithm.

After isolation of the relevant histology, the Otsu algorithm is applied to the section to provide a thresholding limit. Tabulated normalized data can then be viewed with Microsoft Excel after processing with the Perl normalizing script. Data collected with this method was compared to that obtained by visual thresholding alone using a cohort of 30 prostate needle biopsies containing high-grade prostatic intraepithelial neoplasia (HGPIN), the putative precursor of invasive prostatic carcinoma.

Results: We were able to demonstrate a high correlation coefficient with visual telomeric thresholding (R = 0.91) using a Cy3 flurochrome and applying the normalized data and the Otsu algorithm.

Conclusions: A new implementation of the Otsu thresholding algorithm, automated nuclear analysis within the Image J program and a normalizing program allows for rapid, objective and accurate analysis of telomeric fluorescent sections and may prove adaptable to the quantification of telomeric and other FISH signals in a variety of clinical samples.

1538   Effect of Fixatives on Nuclear Protein Extraction and Proteomic Analyses Using Two-Dimensional Protein Electrophoresis
P Kapur, LR Margraf, D Rakheja. University of Texas Southwestern Medical Center, Dallas, TX.

Background: Global protein expression studies are traditionally performed on fresh or freshly frozen tissues and cells. However, the majority of archival material in pathology departments is in the form of formalin-fixed and paraffin-embedded tissues. There is a need to assess the effect of fixatives on protein recovery from tissues and cells.

Design: To avoid heterogeneity of cells within a tissue sample, we performed our study on a cell line. We cultured a Wilms tumor cell line, SK-NEP-1, in complete RPMI 1640 containing 10% fetal bovine serum. Harvested cells were washed with phosphate-buffered saline, and 50 ul each of cell pellet was fixed for 1 hour in 10% neutral buffered formalin, Bouin's fixative, and 90% ethanol. Another 50 ul of cell pellet was frozen at -80 Celsius. Nuclear proteins were extracted from the four cell pellets using ReadyPrep Cytoplasmic/Nuclear Protein Extraction Kit (BioRad) and 20ug of protein from each extract was used for 2-dimensional protein electrophoresis. The final gels were stained with SYPRO Ruby fluorescent dye and imaged using VersaDoc 3000 imaging system (BioRad). The imaged gels were analyzed using PDQuest software (BioRad).

Results: The total amount of nuclear protein extracted from each sample was: 988.41 ug (formaldehyde fixed cells), 1551.44 ug (Bouin's fixed cells), 2094.66 ug (ethanol fixed cells), and 1694.04 ug (unfixed cells). The numbers of protein spots detected by PDQuest software were: 240 (formaldehyde-fixed cells), 460 (Bouin's-fixed cells), 454 (ethanol-fixed cells), and 454 (unfixed cells). Comparisons of proteins spots between fixed and unfixed cells showed that only 74 protein spots from formaldehyde-fixed cells, 208 from Bouin's-fixed cells, and 198 from ethanol-fixed cells matched with protein spots from unfixed cells.

Conclusions: Our study shows that fixation of cells in formaldehyde, Bouin's fixative, and ethanol affects cellular protein profiles. The extra protein extracted from ethanol-fixed cells probably reflects cytosolic protein contamination. Of the three fixatives studied, formaldehyde had the maximum negative effect on absolute protein recovery as well as on qualitative protein profile on 2-dimesnional gels. Paraffin-embedding of formalin-fixed tissues may further worsen global protein profiles of tissues.

1539   Multispectral Image Analysis of Multiplexed Immunohistochemical Stains in Breast Cancer
CA Kerfoot, ME Endlich, RM Levenson. US Labs, Irvine, CA; CRI, Woburn, MA.

Background: Immunohistochemistry has been practiced for over 60 years, but few clinical assays have progressed to detect more than one analyte at a time. Detection and analysis of two or more co-localized antigens by light microscopy have been hindered by the difficulty in discerning and quantifying overlaying chromogens. Performing multi-analyte immunohistochemistry has many potential benefits and applications in the field of drug target evaluation and patient screening, including: 1) determination and quantification of immunoreactivity co-localization; 2) evaluation of spatial relationships between immunoreactive cell types; 3) signal transduction pathway activation studies; 4) reduction in tissue depletion; and 5) decreased reagent utilization. Through the use of multispectral imaging, the absorption pattern of overlapping chromogens can be spectrally unmixed into quantitative individual dye components.

Design: In order to implement this in a clinical setting, a number of parameters were evaluated to determine optimal procedures for accurate and reproducible discrimination of multiple analytes. These factors included spectral analyses using the Nuance(tm) multispectral imaging system and comparisons of commercially available chromogen combinations, order of chromogen development, and chromogen development time.

Results: Spectral analysis allowed the separation of red from brown signals even when they spatiallly overlapped. Development with Vulcan Red followed by 3-3 -diaminobenzidine (DAB) produced approximately equivalent immunoreactivity for each analyte, while development with DAB first decreased the staining intensity for Vulcan Red up to 50% compared to slides stained with Vulcan Red individually. This duplex detection scheme was applied to estrogen receptor (ER, DAB) and progesterone receptor (PR, Red), and the assay was used to analyze variances between ratios of ER/PR immunoreactivity in normal breast epithelia and breast carcinoma. Exclusive expression of ER or PR was common in normal breast epithelia, while breast carcinoma cases that were ER- and PR-positive demonstrated immunoreactivity for both receptors within individual cells.

Conclusions: Multi-analyte immunohistochemistry analyzed by multispectral imaging is a clinically viable technique that holds tremendous potential to further characterize and subtype cancers.

1540   The bDNA Assay (Quantigene™) for Quantification of RNA in Formalin-Fixed Tissues
B Knudsen, A Allen, A Kristal, G McMaster. Fred Hutchinson Cancer Center, Seattle, WA; Genospectra, Fremont, CA.

Background: Formalin-fixation fragments and chemically modifies RNA, reducing the sensitivity and reliability of gene expression measurements by real-time PCR (QPCR) in formalin-fixed paraffin embedded (FFPE) tissues.

Design: To overcome the limitations of the QPCR, the bDNA assay was developed to rely on cooperative hybridization. The principle of the bDNA assay is similar to the ELISA assay. In a sandwich-like design, both capture probes and detection primers hybridize to RNA. The bound RNA is measured by chemiluminescence on a linear scale. We measured six housekeeping genes (beta-actin, GAPDH, RPL32, SDHA, HPRT1 and TBP), which vary in expression levels in 3 tissue preparations [OCT-embedded (OCT), controlled formalin-fixed (cFFPE), and archival formalin-fixed (aFFPE)] with and without prior RNA purification. We calculated intraclass correlations (ICCs) to determine the reliability of duplicate assays (intra-assay reliability), and also to calculate the agreement between assays. All tissues were collected with IRB approval.

Results: The assay characteristics of QPCR and bDNA assay were compared as follows: (1) intra-assay reliability was estimated from duplicate assays in eight radical protatectomies collected between 1993 and 1997. ICCs ranged from 0.897 - 0.974 for QPCR, 0.96 - 0.986 for bDNA assay with purified RNA (pRNA) and 0.977 - 0.993 for bDNA assay with tissue homogenate; (2) inter-assay agreement was determined by measurements of RNA abundance in OCT and cFFPE tissues from the same individual and QPCR measurements in OCT tissues were used as the gold standard; (3) limits of quantification were measured using a limiting dilution approach. While the limit of quantification in the QPCR for the three low expressing genes (SDHA, HPRT1 and TBP) was 30 ng of input RNA, it was 10 - 100 fold lower in the bDNA assay. The development of a novel primer design in the bDNA assay permits measurement of RNA fragment length and cell numbers in tissue homogenates. With these parameters an algorithm for evaluation of RNA quality in archival tissue blocks is being established and will be tested for its utility in the selection of tissue blocks for large cohort studies.

Conclusions: In contrast to QPCR, the bDNA assay does not require RNA purification, reverse transcription and enzymatic amplification. Comparison of the bDNA assay to QPCR indicates that the bDNA assay provides a simpler, more accurate and cost-effective method for RNA measurements in cohorts of archival tissues.

1541   Nine-Color/Eleven-Parameter Flow Cytometry Can Be Utilized in the Clinical Laboratory To Diagnose a Broad Range of Hematolymphoid Neoplasms
SJ Kussick, D Ceniza, BK Oppenlander, TS Barry, AM Gown. PhenoPath Laboratories, PLLC and IMPRIS, Seattle, WA.

Background: We investigated the feasibility of using a three-laser, nine-color, Becton Dickinson (BD) LSRII flow cytometer in the routine evaluation of clinical specimens for leukemia/lymphoma immunophenotyping, by evaluating normal peripheral blood and 15 hematolymphoid cell lines.

Design: The three lasers, and the fluorochromes excited by each laser, were as follows: 405 nm (violet) laser - Pacific Blue; 488 nm (blue) laser - FITC, PE, PE-Texas Red, PE-Cy5, and PE-Cy7; and 633 nm laser - APC, AlexaFluor 700, and APC-Cy7. With the exception of a custom-conjugated CD38-APC-Cy7 antibody, the antibodies used were commercially available. Both surface and cytoplasmic staining were performed, depending on the cellular localization of the antigen of interest. 50,000-100,000 cellular events were typically collected per tube. The cell lines included: 1. SUP-B15 (B-lymphoblastic); 2. Raji (Burkitt lymphoma); 3. RL (follicular lymphoma); 4. Granta (mantle cell lymphoma); 5. Jeko-1 (mantle cell lymphoma); 6. Bonna-12 (hairy cell leukemia); 7. NCI-H929 (plasma cell myeloma); 8. MOLT-4 (T-lymphoblastic); 9. Jurkat (T-lymphoblastic); 10. CCRF-HSB-2 (T-lymphoblastic); 11. Karpas 299 (anaplastic large cell lymphoma); 12. NB-4 (acute promyelocytic leukemia); 13. MEG-01 (acute megakaryoblastic leukemia); 14. MV-4-11 (acute biphenotypic leukemia); and 15. K562 (chronic myeloid leukemia in blast crisis).

Results: Flow cytometric analysis using BD's FACSDiva software yielded high quality data from normal blood and all 15 cell lines, demonstrating the expected lineage-specific antigens. When several cell lines were "spiked" into normal blood at concentrations of less than 1% of the leukocytes, the abnormal cell populations were readily identified.

Conclusions: Nine-color/eleven-parameter flow cytometry using the BD LSRII, a traditional research instrument, is feasible in the clinical laboratory. The increased number of antigens evaluated simultaneously allows more efficient use of small amounts of diagnostic material compared to traditional 3-color and 4-color flow cytometry, and is well-suited to detect very small abnormal cell populations in a background of normal cells.

1542   The Role of Core Biopsy in the Evaluation of Spleen Pathology
JI López, JL del Cura, R Zabala, FJ Bilbao, A Gaafar, MV García-Menoyo, A Fdez-Larrinoa. Basurto Hospital, Bilbao, Spain.

Background: Core biopsy (CB) has not been traditionally recommended in the study of spleen nodules due to the supposed fragility of this organ leading to a high risk of post-CB complications, mainly haemorrhage and/or rupture. Actually, there are very few published studies on this topic. The aim of this work is to analyse our experience with this technique in terms of diagnostic accuracy and risks.

Design: The series includes 13 patients who presented solid spleen nodules (11 cases) or diffuse splenomegaly (2 cases) on imaging studies (CT, MR, sonography). Pathologic images were detected either in the context of a known disease or appeared *de novo* during routine exams, and were biopsied under ultrasound control with 18G BioPince® needles. Ultrasound exams were done in all cases to identify post-CB complications. Splenectomy was performed in 5 cases.

Results: Males predominated in the series (9M/4F). Average age was 61 years (range,

25-93). Malignant lymphomas were the most common pathology (4 diffuse large B-cell lymphomas, 2 follicular lymphomas, 1 Hodgkin's disease, 1 B-cell lymphoma, NOS). In addition, there was 1 littoral-cell angioma, 1 well differentiated neuroendocrine carcinoma, metastatic, and 1 haemangioma. The remaining two cases showed congestive features, and the supposed spleen involvement by Hodgkin's disease was ruled out. Clinical/haematological data and/or splenectomy confirmed the CB diagnosis in all cases. On follow-up, there were not complications related to CB.
Conclusions: CB is a safe and efficient method in the diagnosis of spleen nodules and splenomegaly, and could be consided in the routine diagnostic algorithm of these lesions. Among them, malignant lymphoma is the commonest diagnosis, but other primary tumours, and even metastases, may be succesfully identified.

1543 An Immunohistochemical Assessment of Rabbit Monoclonal Antibodies Compared to Their Mouse Monoclonal and Rabbit Polyclonal Counterparts

S Lau, J Tao, JX Zhao, R Wu. Zymed Laboratories, A Division of the Invitrogen Corp, South San Francisco, CA.
Background: The most commonly used primary antibodies have been mouse monoclonal and rabbit polyclonal (antisera) antibodies. Mouse monoclonal antibodies (MsMAb) are famed for their ability to produce specific staining (with less sensitivity than rabbit polyclonal antibodies). In contrast, rabbit polyclonal antibodies (RbPAb) are renowned for their ability to produce sensitive staining (with less specificity than MsMAbs). The development of rabbit monoclonal antibodies (RbMAb) is fairly new and has only recently become commercially available for diagnostic immunohistochemistry. It is thought that RbMAbs retain the sensitivity of RbPAbs while exhibiting the specificity of MsMAbs. Studies have shown that some RbMAbs may be better predictors of prognosis than their standard counterparts.
Design: Formalin-fixed, paraffin-embedded sections of various carcinoma and normal tissue samples were used in this comparison of RbMAbs to their standard MsMAb or RbPAb counterparts. Antibody pairing was executed as follows:

Target used	Rabbit Monoclonal Antibodies		Standard Counterparts		Tissue samples mainly
	Catalog No.	Clone	Antibody	Clone	
CD3	08-1450	ZYM 14	pRbAb	N/A	Gastric carcinoma
CD5	08-1451	ZYM 15	mMsAb	4C7	Tonsil
CD8	08-1452	ZYM 16	mMsAb	C8/144B	Tonsil
CD23	08-1453	ZYM 17	mMsAb	1B12	Tonsil
CD79a	08-1454	ZYM 18	mMsAb	JCB117	Tonsil
COX-2	08-1455	ZYM 19	mMsAb	CX-294	Colon carcinoma
Cyclin D1	08-1449	ZYM 13	mMsAb	DCS-6	Mantle cell lymphoma, breast carcinoma
ER	08-1447	ZYM 11	mMsAb	6F11	Breast carcinoma
PR	08-1446	ZYM 10	mMsAb	PgR 636	Breast carcinoma

Immunohistostaining was done manually using the Histostain®-Plus, SuperPicTure™, and DAB kits (Zymed-Invitrogen). All immunohistostaining performed followed parallel protocols and recommended pretreatments. Antibodies were diluted according to manufacturers' recommended titers.
Results: Each RbMAb outperformed its counterpart in terms of staining intensities and level of background. In all cases, the RbMAbs produced stronger staining than their counterparts with no obvious background.
Conclusions: The RbMAbs appear to possess the specificity of a MsMAb while preserving the sensitivity of a RbPAb. All the RbMAbs exhibited higher sensitivity than their MsM counterparts. RbMAbs appear to be suitable alternatives to MsMAbs and RbPAbs.

1544 A Chromogenic In Situ Hybridization (CISH) Technique for Visualizing Telomeric DNA in Fixed Tissue Sections

AK Meeker, JL Hicks, E Smearman, AM De Marzo. Johns Hopkins University School of Medicine, Baltimore, MD.
**Background:** Telomeres form protective capping structures composed of variable numbers of telomeric DNA repeats at the ends of the chromosomes. Telomeric DNA is lost during cell division and as a result of unrepaired oxidative damage. Critical shortening of telomeric DNA destabilizes telomeres, thereby instigating chromosomal instability. Dysfunctional telomeres have been implicated as a causal factor in malignant transformation as well as other age-associated pathologies. Current tissue-based research makes use of Fluorescent in situ hybridization (FISH) methods for direct telomere length analysis. Here we describe a method for performing such studies using chromogenic rather than fluorescent detection.
Design: We hybridized a Cy3-labelled peptide nucleic acid (PNA) probe complementary to the telomeric repeat sequence (TTAGGG) to formalin-fixed paraffin-embedded tissue sections and fixed cells. The PNA probe was then visualized using a specific anti-Cy3 antibody and a commercial HRP/DAB chromogenic detection system (DAKO Envision kit), followed by hematoxylin counterstaining. Slides were then visually assessed by standard light microscopy.
Results: Telomeric signals were readily apparent as punctate dots within the nuclei of human and mouse cells (e.g. Figure a: cultured mouse fibroblasts). In human prostate tissues obtained from radical prostatectomy for prostate cancer, the invasive malignant component displayed markedly reduced signals compared to surrounding normal prostate glands and lymphocytes (Figure b).
Conclusions: Chromogenic methodology allows telomere length assessment to be done using standard light microscopy. This new method will facilitate a broader application of telomere length analysis for answering basic questions regarding telomere length changes in pathology research.
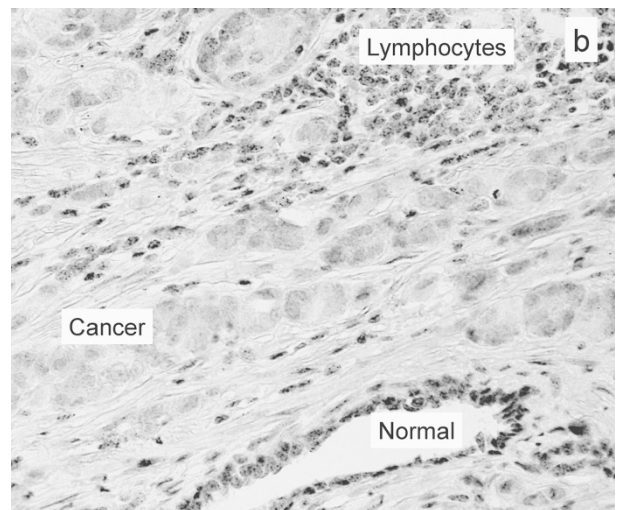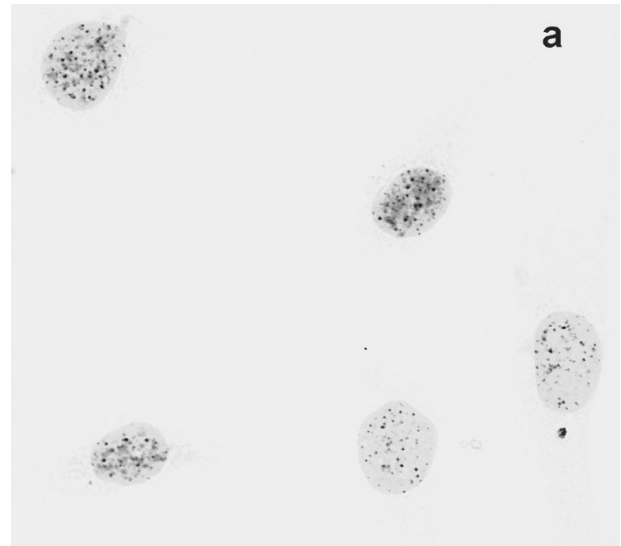
1545 Identification of Qualitative and Quantitative Alterations in the Mitochondria of Enriched Cell Populations between Matched Normal and Malignant Colonic Tissue

WD Mojica, LA Hawthorn, BK Stefanick, X Fang. University at Buffalo; Roswell Park Cancer Institute, Buffalo, NY.
Background: Mitochondrial DNA may potentially serve as a sentinel biomarker for neoplasia. Its well characterized genome, high copy number and overall stability make it an attractive target for molecular analysis relative to nuclear DNA. Initial studies on colorectal mitochondrial mutations were performed predominatly on cell lines. The feasibility of detecting alterations in the copy number of mitochondria and the mitochondrial genome from colorectal clinical specimens was assessed using the technique of manual exfoliation coupled to immunomagnetic bead separation.
Design: Normal and neoplastic colonic epithelial cells from a hemicolectomy specimen were procured by manual exfoliation and underwent positive selection by using immunomagnetic beads (Dynal Epithelial Enrich, Invitrogen, Brown Deer, WI). One half of the enriched cell population was subjected to cell lysis followed by DNA precipitation and isolation; the other half was fixed in PBS with 1% glutaraldehyde. The polymerase chain reaction was performed on the DNA and the amplified product probed unto an Affymetrix MitoChip. The results were compared to the Revised Cambridge Reference Sequence. The fixed cells were sectioned, viewed under an electron microscope, and the number of mitochondria in 10 fields collated.
Results: Manual exfoliation with immunomagnetic bead separation resulted in the enrichment of colonic epithelial cell populations. Four previously unreported homoplastic mutations (G3316A, G8545A, T10873C and G11600A) and one heteroplastic mutation (A13901 A/C) were identified in the mitochondrial DNA of the

neoplastic cells. 50 single nucleotide polymorphism were noted. Though not statistically significant, the average number of mitochondria in a 10,000X field from normal cells was 7.4 and 11.1 from neoplastic cells.

Conclusions: Cell enrichment is necessary to establish baseline numbers of mitochondria per cell and define the presence of homplastic or heteroplastic mitochondrial mutations. Relative to matched normal colonic epithelial cells, neoplastic colonic epithelial cells demonstrated an increased copy number of mitochondria per cell and 4 homoplastic and 1 heteroplastic mutation. These results validate the feasibility of this approach in the identification of mitochondrial mutations as potential biomarkers in clinical resection specimens of colorectal cancer.

1546 Proteomics of Tissue Samples Prepared by a Molecular-Friendly Fixation and Processing System

M Nassiri, M Nadji, V Vincek, AR Morales. University of Miami Miller School of Medicine, Miami, FL.

Background: Current tissue fixation and processing methods for clinical specimens have severe limitations for proteomic studies. This is mainly due to the type of reagents used in the conventional fixation and processing. We have developed a standardized formalin-free tissue fixation and processing system that includes molecular-friendly reagents and automated instruments. The reliability of this system in preserving macromolecules for proteomic studies in paraffin tissue was evaluated.

Design: Parallel slices of mouse or human tissue were fixed in formalin and in UMFIX (Molecular Fixative, Sakura, Torrence, CA) for periods of time ranging from 1hr to 24 hr. Samples were then processed by a microwave-assisted tissue processor (Xpress; Sakura). Total proteins were isolated from control fresh tissue, fixed tissues and paraffin-embedded processed specimens. Two dimensional electrophoresis and SELDI-TOF (IMAC30-Cu and CM10 chips, Ciphergen, Fremont, CA) was performed as well as Western Blot for 34 proteins and their phosphorylated variants. In addition, immunohistochemistry for 70 commonly used antigens was performed on sections from the same tissue blocks.

Results: High-resolution protein profiles were obtained from tissues processed by the new fixation and processing method using 2D gel and SELDI-TOF. In contrast, no such pattern was observed in formalin fixed samples. Similar profiles could also be obtained following storage of paraffin blocks up to 6 months at room temperature using the new method. Antigen preservation by western blot and immunohistochemical studies was also superior in the tissues processed by the molecular-friendly system.

Conclusions: The new formalin-free fixation and processing system has the potential to serve as the standard platform for proteomic studies of human tissue.

1547 The Effect of Storage on the Antigen Expression of Tissue Microarray Slides

KC O'Reilly, MW Datta, AJ Kahler, MB Amin, AA Kajdacsy-Balla. Emory University Hospital, Atlanta, GA; Medical College of Wisconsin, Milwaukee, WI; University of Illinois-Chicago, Chicago, IL.

Background: Tissue microarrays (TMAs) offer the promise of maximizing specimen use through the production of slides each containing hundreds of individual tissue cores. However, the production and storage of TMAs for optimal use has been an area of concern. Recent studies have identified loss of antigen expression in tissue microarray slides after storage at room temperature. Even storage periods of a few days may alter antigen expression. We sought to determine if the storage of tissue microarray slides at 4C and under various conditions would improve antigen preservation.

Design: We constructed TMAs containing 300 0.6 mm cores of benign prostate tissues. The tissue was placed in a microarray block and sequential slides were prepared and either 1) immediately used for immunohistochemistry (IHC), 2) stored for two months at 4C in a vacuum dessicator, 3) stored for two months at 4C in a vacuum dessicator in the dark, or 4) dipped in paraffin and stored for two months at 4C in a vacuum dessicator in the dark. Slides were then used for IHC. Markers included high molecular weight cytokeratin (HMWCK), p53, p27, and androgen receptor (AR). After staining slides were scored for tissue loss and the presence of antibody staining (presence/absence). Staining intensity and background staining were measured on a 0 (no staining) to 3 (strong brown staining) scale. Calculations were performed for general tissue and staining characteristics, along with signal to background values.

Results: No significant differences were noted for tissue loss or positive antibody staining for any of the storage techniques compared to freshly prepared TMA slides. Of note, there was reduced intensity of staining for p53 and AR when slides were stored, but background non-specific staining was also reduced. HMWCK and p27 did not demonstrate decreased staining intensity. Signal to background ratios were statistically similar across all groups, ranging from 1.61 to 1.87.

Conclusions: Storage of slides at 4C provides sufficient protection for IHC studies. While some loss of staining intensity can be seen after two months, the decreased background staining allows retention of high signal to noise ratios. Further studies could be performed to determine if the quality of staining would be maintained over longer storage periods. Storage at 4C under dessication provides similar protection without the need for cumbersome paraffin coating of slides or storage in the dark.

1548 Analysis of a Five-Item Questionnaire and a Self-Assessment Module for Teaching Neuropathology during Pathology Residency Training

S Parikh, T Tihan. UCSF School of Medicine, San Francisco, CA.

Background: ACGME competencies include practice-based learning and medical knowledge. Despite the availability of general principles and methods, specific tools for testing these competencies in pathology training are currently not available. Most performance evaluations currently employed in pathology departments have not been adequately tested for validity and reliability.There is a need to develop practical, reproducible, and standardized competency assessment methods.

Design: In an attempt to develop a practical and effective assessment method we generated a five-item questionnaire and interactive multiple choice question self-assessment module for neuropathology teaching. The modules aim to test practice-based learning and medical knowledge. Participants of the anatomic pathology program were given the questionnaire and self-assessment module, multiple times over the course of the academic year for a minimum of five times. The appropriateness of answers was evaluated on specific cases assigned in each test. Subjects were also tested using randomly selected multiple choice questions compiled from a question databank.

Results: Twenty-six residents, 16 fellows, and seven rotating medical students were tested for a minimum of five times during training. The mean values on the first evaluation were 26.8% (medical student), 49.5% (resident), and 56.3% (fellow), this increased to 71.4%, 77.3 % and 80.8% respectively by the fifth evaluation. There was a significant difference in percent appropriate answers in all groups over time, and the improvement was most pronounced in medical students (p<0.01). Differences among mean scores of neuropathology fellows and mean scores of all other groups remained statistically significant throughout the five evaluations, except for the resident group with longer than 2 years of surgical pathology experience at the time of the fifth evaluation.

Conclusions: A simple 5-item questionnaire demonstrates sufficient reliability and validity for practical use in an institution. Self-assessment modules, utilizing multiple choice questions may assist residents in learning the subject matter. Further studies are required in order to determine the applicability of these assessment tools to other subspecialties in pathology, different programs, and institutions.

1549 Availability and Quality of Paraffin Blocks Identified by the Shared Pathology Informatics Network (SPIN): A Multi-Institutional Study

AA Patel, D Gupta, D Seligson, EM Hattab, U Balis, TM Ulbright, JJ Berman, JR Gilbertson, MJ Becich, AV Parwani, Shared Pathology Informatics Network. Univ of Pittsburgh, Pittsburgh, PA; UCLA, Los Angeles, CA; Indiana Univeristy, Indianapolis, IN; Harvard Univ, Boston, MA; DCTD, NCI/NIH, Rockville, MD.

Background: The NCI Shared Pathology Informatics Network (SPIN, http://spin.nci.nih.gov) is a multi-institution consortium based on coding of clinical reports that allows investigators to locate human biospecimens for research. Study objectives were to determine (1) the availability and quality of paraffin blocks identified by the SPIN tool or local lab information systems (LIS) and (2) the percentage of cases that had tumor available for research purposes.

Design: Four centers evaluated path reports (1990-2005) for common (Phase I) and uncommon tumors (Phase II) to determine the percentage of cases where suitable tissue blocks with tumor were available. Each site generated a list of 100 common (25 cases each of prostate, breast, lung, colon) and 100 uncommon tumors (25 cases each of adrenal cortical carcinoma, gastrointestinal stromal tumor, adenoid cystic carcinoma, mycosis fungoides) using a combination of Tumor Registry, LIS and/or SPIN-related tools. Pathologists identified the slides/blocks with tumor and noted first 3 slides with largest tumor.

Results: For Phase I, each institutions retrieval rates(all blocks) were 83%(A), 95%(B), 80%(C), and 98%(D). Retrieval rate (tumor blocks) from all centers for common tumors was 73% with a mean largest tumor size of 1.49cm; Retrieval (tumor blocks) was highest for lung(84%) and lowest for prostate(54%). For Phase II, each institutions retrieval rates(all blocks) were 78%(A), 73%(B), 67%(C), and 84%(D). Retrieval rate (tumor blocks) from all centers for uncommon tumors was 66% with a mean largest tumor size of 1.56cm; Retrieval (tumor blocks) was highest for GIST(72%) and lowest for adenoid cystic carcinoma(58%).

Conclusions: High retrieval rates(all blocks) are shown for acquiring both common(89%) and uncommon tumors(76%), irrespective of the retrieval method. Assessment shows the feasibility of using a SPIN query tool to search for archival tissue. It assures and highlights the usefulness of archival material for obtaining both common and rare tumors. Future studies will be directed towards utilizing the SPIN query tool uniformly by all four centers. Work was supported by NCI grant U01 CA 091338 from SPIN.

1550 The NCI Cooperative Prostate Cancer Tissue Resource:Informatics Support for a Multi-Institute Biorepository

AA Patel, JR Gilbertson, AV Parwani, R Dhir, MW Datta, R Gupta, JJ Berman, MJ Becich, Cooperative Prostate Cancer Tissue Resource. University of Pittsburgh, Pittsburgh, PA; Emory University, Atlanta, GA; DCTD, NCI/NIH, Rockville, MD.

Background: Advances in molecular biology and growing requirement for biomarker validation studies have generated a need for tissue banks to provide large numbers quality controlled tissue samples with standardized clinical annotation. The NCI Cooperative Prostate Cancer Tissue Resource (CPCTR) is a distributed tissue bank that provides thousands of clinically annotated prostate cancer specimens to the researchers. It comprises four academic centers. Here we describe the CPCTR information management system architecture, CDE development, query interfaces, data curation and quality control.

Design: At each center, using an Access database, data managers review and extract data for each case using 145 clinical, pathological, and inventory common data elements (CDEs) developed by the Resource and manage linkage to case identifiers in a standardized method. Quality control audits of clinical data are conducted by independent qualified individuals at regular intervals. Methods for calculating biochemical recurrence based on collected pre/post diagnostic PSA values is implemented. De-identified data is sent to a central Oracle database allowing mining of the data by users in three levels with increasing levels of specificity and de-identification. The specimens and information are de-identified before being provided to researchers.

Results: Since July 2003, CPCTR offers over 6000 cases (38000 blocks) of highly characterized prostate cancer tissue specimens, including tissue microarrays. As of September 2005, the Resource website (www.prostatetissues.org) had over 5700

website hits and over 1600 hits for its Public database. Received over 125 tissue requests of which 44 have been approved and fulfilled. In addition, the Resource has demonstrated how the TMA Data Exchange Specification is implemented in a prostate cancer TMA and created a program for calculating PSA recurrence.

Conclusions: Building a biorepository infrastructure that meets todays research activity needs involves major time and input of many individuals from diverse disciplines. Lending its experiences, CPCTR can assist in the development of a virtual tissue bank with the ability to collaborate and provide valuable tissue resources for research initiatives such as SPORE's and collaborative groups. This work is supported by NCI grant U01 CA 86735.

1551 Addressing the Issue of Discordance between Techniques: Analysis of Chromosome 1 Abnormalities in Renal Oncocytoma by Conventional Cytogenetics, FISH and LOH
MM Picken, B Chyna, JM Lee. Loyola University Medical Center, Maywood, IL.
Background: The interpretation of molecular studies poses a significant problem, partly because no "gold standard" is available for comparison. We sought to compare the results of 3 techniques using the evaluation of chromosome (chr) 1 in renal oncocytomas (RO) as a model. A subset of RO has been shown to lack chr 1/1p by conventional cytogenetics (CC). It has been proposed that this loss of 1/1p is associated with the loss of a tumor suppressor gene. Previously, we compared CC & FISH in the evaluation of chromosome 1. We have now extended these studies to incorporate the evaluation of loss of heterozygosity (LOH).
Design: We analyzed chr 1 in RO by CC, FISH & LOH. CC was performed as previously reported (*JUrol* 2004,171:602). For FISH, a LSI 1p36/LSI 1q25 dual color probe set from Vysis, Inc was used. LOH analysis was carried out using 3 microsatellite markers (D1S508, D1S199, D1S2734) and a PCR based assay. Paraffin sections from tumor and adjacent normal tissue were studied. DNA extraction, end-labelling & PCR amplification were performed as previously described (*BMC Clinical Pathology* 2003,3:6). DNA samples, heterozygous for any of the 3 loci, were considered informative, whereas homozygotes were deemed "non-informative".
Results: 16 tumors were evaluated by all 3 techniques. In 2 cases, LOH could not be interpreted. In 7 cases with -1/1p loss by CC & FISH, there was also LOH in all 3 loci in all tumors. 4 tumors were disomic by CC & FISH. However, in 2 of these tumors there was LOH in D1S508 (x2) and D1S2734 (x2), 2 loci showed no deletion & 3 markers were non-informative. In 3 tumors disomic for chr 1 by CC & monosomic by FISH, there was LOH at D1S508 (x1), D1S199 (x1) & D1S2734 (x3). In 1 tumor, D1S508 showed no LOH, while 3 remaining markers were non-informative. There was excellent correlation between all 3 techniquens in tumors with loss of 1/1p. In 3 cases of discordance between CC & FISH, LOH studies corroborrated the FISH results, suggesting that stromal overgrowth may have contributed to the normal karyotype observed by CC. In 4 tumors, where CC & FISH failed to demonstrate abnormalities, LOH was demonstrated in several loci, suggesting that the FISH & LOH probes may have hybridized to non-overlapping regions of the chr.
Conclusions: There was excellent correlation between all 3 techniques in 9 tumors. In 3/3 cases LOH studies were helpful in explaining the discordance between CC and FISH. However, the detection of LOH in 2 tumors disomic by CC & FISH, requires additional studies.

1552 Comparison of Polyclonal (DakoCytomation) and Monoclonal (T595, Novocastra) Antibodies in the Identification of Gastrointestinal Stromal Tumors and Other CD117 (c-kit)-Positive Neoplasms
AC Popp, JR Goldblum, C Cohen, AL Folpe. Emory University Hospital, Atlanta, GA; Cleveland Clinic, Cleveland, OH.
Background: CD117 (c-kit) is a cell surface tyrosine kinase receptor present on normal mast cells, germ cells and the interstitial cell of Cajal. CD117 is a useful marker of GIST, as well as mast cell tumors (MC), adenoid cystic carcinomas (ACC) and seminomas (SEM). CD117 expression is of prognostic and predictive significance, as imatinib mesylate (Gleevec) is used to treat CD117-positive GIST. The Dako polyclonal antibody to CD117 is most widely utilized, and is recommended for entry of GIST patients into clinical trials. Recently, a number of different monoclonal antibodies to CD117 have become available. We compared a polyclonal CD117 antibody to a newer mAb in GIST, MC, ACC and SEM.
Design: 40 GIST, 5 MC, 5 ACC, and 5 pure SEM were immunostained for CD117, using the DakoCytomation polyclonal antibody and the T595 monoclonal antibody (Novocastra), with heat induced epitope retrieval and the DAKO Envision+ and Envision systems, respectively. Cases were scored as negative - 0, 1-24% - 1+, 25-50% - 2+, >50% - 3+.
Results: Cases (+) with either antibody: GIST (28/40, 70%), ACC (4/5, 80%), MC (5/5, 100%), SEM (5/5, 100%).

Percentage of Cases Positive with Each Antibody

	+ by both (%)	+, pCD 117only (%)	+, mAb T595only (%)	2-3 +, either (%)	2-3 +, both (%)	2-3 +, pCD117 only (%)	2-3 +, mAb T595 only (%)
GIST	21 (75)	6 (21.4)	1 (3.6)	27 (96.4)	20 (71.4)	6 (21.4)	0 (0)
ACC	4 (100)	0 (0)	0 (0)	4 (100)	3 (75)	1 (25)	0 (0)
MC	5 (100)	0 (0)	0 (0)	1 (100)	5 (100)	0 (0)	0 (0)
SEM	5 (80)	0 (0)	0 (0)	5 (100)	3 (60)	5 (100)	0 (0)

Conclusions: pCD117 and mAb T595 are equally sensitive in the identification of MC, ACC and SEM However, in GIST, pCD117 is significantly more senstiive. Additionally, pCD117 results in considerably more "robust" staining than does T595, with many more "2-3+" cases; this may be very valuable in the setting of small biopsies. Thus, pCD117 should be used instead of T595 in the routine screening of suspected GIST and other CD117-positive tumors. However, very rare GIST are positive with T595 but not pCD117, and both antibodies should be utilized prior to diagnosing "CD117-negative" GIST. Comparison of T595 to other CD117 mAb's is warranted.

1553 Color Conversion of Enzyme Metallographic Signals: A New Ultrasensitive Method for Chromogenic Signal Generation
RD Powell, VN Joshi, JF Hainfeld, K Das, R Lounsbury, J Pettay, RR Tubbs, R Levenson. Nanoprobes, Inc, Yaphank, NY; Cleveland Clinic Foundation, Cleveland, OH; CRI, Inc, Woburn, MA.
Background: Enzyme metallography has achieved both ultrasensitive, high-resolution detection and localization of individual gene copies by conventional brightfield microscopy in situ hybridization, and highly sensitive and specific histochemical staining of target proteins in paraffin-embedded tissue sections. However, its application to spectral imaging and other automated imaging methods has been limited because the black signal does not give an identifiable spectrum, and differentiation of enzyme metallographically stained targets by color would enable simultaneous characterization of more targets. We therefore investigated methods for the conversion of enzyme metallographic signals to a chromatically distinct color.
Design: Unstained sections of invasive ductal carcinoma of the breast from different specimens were first evaluated by in situ hybridization with enzyme metallographic detection for HER2 gene status. When enzyme metallographic staining was complete, the sections were treated with a bleaching agent followed by a two-component staining mixture, resulting in conversion of the black enzyme metallographic signal to a blue color. We also investigated this approach for immunohistochemistry using tonsil sections stained with murine monoclonal antibody L26 spedific for CD20 followed by secondary enzyme metallography development. The resulting black stain was then converted to a blue color using the same sequence of bleaching followed by treatment with the two-component color conversion mixture used with the HER2 gene signal.
Results: In both systems, complete conversion of the black enzyme metallographic signal to a distinctive deep blue color was observed. The blue color was equal in intensity to the black enzyme metallographic signal, afforded a very similar degree of detection sensitivity and localization resolution, and could be visualized using a conventional brightfield microscope without oil immersion. Background staining was very low in both systems.
Conclusions: Generation of a colored, spectrally discrete signal from enzyme metallographic stain was successfully achieved for in situ hybridization (ISH) and immunohistchemical (IHC) staining, and both the sensitivity and resolution of the enzyme metallographic stain are preserved. Using this method, the advantages of enzyme metallographic staining may be applied to spectral imaging and image analysis.

1554 FISH on Paraffin-Embedded Lymphoid Tissue Sections Is Automated, Fast and a "Value-Added" Tool in the Diagnosis and Prognosis of B-Cell Lymphoma
K Reichard, A Corn, B Hall, J Hozier. University of New Mexico, Albuquerque, NM; TriCore, ABQ, NM.
Background: Certain recurrent cytogenetic abnormalities are diagnostic of a specific neoplasm and may portend prognosis. This is particularly true for B-cell lymphomas. As conventional cytogenetics may not reveal a neoplastic clone, and traditional material (unfixed specimen) for FISH may be unavailable, there is diagnostic and prognostic value for FISH on fixed tissues (FT). Thus, we determined if 3 translocation FISH probes [(11;14) mantle cell lymphoma (MCL), (14;18) follicular lymphoma (FL), (8;14) Burkitt lymphoma (BL)] could yield interpretable signal patterns on FT, be scored in an automated, unbiased fashion, and provide fast results that are clinically, diagnostically and prognostically significant
Design: Paraffin blocks from 20 cases of non-neoplastic lymph nodes, 12 BL, 8 FL and 14 MCL were retrieved from UNM pathology files. Cases in several fixatives (formalin, B5 and AZF) were chosen for comparison. Diagnoses were confirmed by review of H&E slides, immunohistochemistry, flow cytometry and cytogenetics. *FISH protocol:* 4 micron unstained FT sections were probed with dual color (t(11;14), t(14;18)) or tricolor t(8;14) dual fusion probes according to the standard pretreatment and hybridization protocols for Her2 (Vysis, Inc. ©). Each probe was run on 20 normal samples for validation, in addition to the specific neoplastic specimens. Nuclei were counterstained with DAPI. *FISH analysis:* MetaSystems© automated FISH analyzer (Altlussheim, Germany) was used for analysis. Two different signal classifiers were used and optimized for signal detection. Areas of tumor were identified (AC, BH) and cell images with signal patterns captured. After correction for cell size in each case, the data for # of fusion signals was presented in histogram format. Cases were deemed positive with increased fusion signals relative to normal controls.
Results: 1) MetaSystems© determines presence or absence of increased fusion signals in positive and negative cases of lymphoma, respectively 2) Automated, unbiased, no manual scoring inaccuracy 3) Fast, 48 hour TAT 4) Variety of fixatives can be used, although formalin is superior 5) Clinically valuable
Conclusions: FISH on fixed tissue is a "value-added" tool in the diagnosis and prognosis of B-cell lymphoma. In addition, it is automated, reproducible and fast. Such analysis provides crucial information, particularly if other specialized testing modalities are unavailable or suboptimal.

1555 Immunophenotypic Attributes of Reactive Circulating γδ T-Cells and Clinical Associations
AC Roden, WG Morice. Mayo Clinic, Rochester, MN.
Background: γδ T-cells represent a small proportion (1-5%) of circulating T-cells in healthy individuals. Due to the paucity of these cells in normal peripheral blood there are few descriptions of their immunophenotype. Furthermore, the function of these cells remains obscure and conditions leading to a reactive increase in circulating γδ T-cells are poorly understood. The results of flow cytometric immunophenotyping (FCIP) studies were reviewed in a series of 64 cases with a reactive γδ T-cell lymphocytosis. In addition, clinical data were reviewed to determine conditions associated with this finding.

Design: Data were reviewed from 352 peripheral blood specimens in which T-cell FCIP studies were performed. A 4-color FCIP strategy was employed using fluorochrome conjugated antibodies to the T-cell and NK-cell associated antigens CD2, CD3, CD4, CD5, CD7, CD8, CD16 and γδ T-cell receptor heterodimers. 64 (18%) cases in which γδ T-cells comprised either >5% of the total lymphocytes or/and had an absolute count of >200 x 10⁶ cells /μL were selected for further study. Cases in which either the cytologic features or phenotypic and molecular genetic findings were suggestive of T-cell malignancy were excluded.

Results: The γδ T-cell levels in the 64 cases are summarized in Table 1.

Number and % of γδ T-cells

	Median	Range
% Total Lymphs	7.4	2.4 to 72.6
% T-cells	9.4	2.7 to 42.2
Cells per μL	220	37 to 1,631

Results of FCIP are shown in Table 2.

Antigen expression by γδ T-cells (number of cases, total=64)

Antigen	Complete Loss	Partial Loss	Dim	Expressed	Bright
CD2				64	
CD3			1	57	6
CD5	12	6	1	44	1
CD7			4	60	

Most commonly observed were aberrancies of CD5 expression with either partial (n=6) or complete (n=12) loss seen. CD16 coexpression was also frequent (n=21), in many of the CD16 positive cases abnormalities of CD5 expression were also present (n=14). Clinical data were available from 36 patients; in 28 there were one or more associated conditions including: infection/inflammatory disease (n=18), autoimmune disease (n=10), lymphoproliferative disorder (n=4) and splenectomy (n=3). No correlation was identified between the phenotype of γδ T- cells and clinical findings.

Conclusions: Slight reactive increases in circulating γδ T-cells are relatively frequent and appear to be associated with immune system activation and splenectomy. Furthermore, these cells can exhibit immunophenotypic features associated with neoplastic conditions such as T-LGL leukemia. For this reason, caution should be exercised in interpreting the significance of this finding in the absence of clinical association.

1556 Quantitative Image Analysis-Based Prediction of Prognosis in Early Stage Breast Cancer Using the TriPath Oncology ProExBr System
JS Ross, AB Boguniewicz, MS Ross, CE Sheehan. Albany Medical College, Albany, NY.

Background: Recent reports document a growing list of biomarkers and commercial assays that demonstrate varying utility in the risk stratification of early-stage breast cancer patients for disease recurrence and/or death. We tested the five biomarker panel (Tripath Oncology ProEx Br, Durham, NC) containing the genes SLPI, E2F1, c-src, p21ʳᵃˢ and PSMB9 for its ability to predict prognosis in lymph node negative breast cancer.

Design: 246 formalin fixed, paraffin embedded archival specimens of invasive ductal carcinoma breast cancer with a minimum five year clinical follow-up were employed in this retrospective study. Specimens were processed via standard IHC protocols using the appropriate monoclonal antibody (ProEx Br, TriPath Imaging Inc.) on a Dako Autostainer (Dakocytomation). The labeling intensity of the slides was quantitatively scored by the IHIS image analysis system (TriPath Imaging) that quantitates subcellular immunostaining intensity and distribution using brightfield microscopy.

Results: Quantitative image analysis of this biomarker panel risk stratified this LNN cohort. In Table 1, the performance of the biomarkers collectively and in conjunction with standard clinico-pathologic parameters was assessed by multivariate Cox proportional analysis. Quantitative image analysis of this biomarker panel risk stratified this LNN cohort. Using Kaplan-Meier plot the risk of recurrence or death increases from approximately 40% to approximately 70% when any two or more of the 5 marker panel are positive (p=0.0078).

Conclusions: This data supports the potential utility of this 5 gene panel to risk stratify node negative breast cancer patients. The 5 biomarker group achieved independent prognostic utility in assessing disease recurrence including a significant reduction in survival rates when two or more of the 5 biomarkers were positive.

Marker	P value	Hazard Ratio
SLPI (individual)	0.0155	2.15
c-src (individual)	0.0321	1.82
Any 1 or more of 5 (SLPI, E2F1, c-src, PSMB9)	0.0498	1.33
Any 1 or more of 4 (SLPI, E2F1, c-src, PSMB9)	0.0223	1.41
Any 1 or more of 3 (SLPI, E2F1, c-src)	0.0068	1.57
1 or more of 3 (SLPI, E2F1, c-src) with other factors (age, tumor size)	0.0034	2.36

1557 Detection and Analysis of Phosphorylated Signaling Proteins in Solid Tumour Fine Needle Biopsies
J Schwock, J Ho, D Hedley, W Geddie. University of Toronto, Toronto, ON, Canada; University Health Network, Toronto, ON, Canada.

Background: The application of molecular targeted therapeutics is expected to cause down- or up-regulation of the respective cellular signaling pathway(s). This may be monitored during treatment of solid tumours by sequential biopsies. Fine needle biopsy (FNB) sampling of tumours is inexpensive, atraumatic, feasible at anatomic sites not suitable for large core biopsy, and easily repeated during treatment. The optimal means of detection and analysis of phosphorylated proteins, however, has not been defined for specimens of this type. Using murine tumour xenografts we have tested different ways of preparing FNB samples for immunohistochemical/immunofluorescence-based analysis.

Design: Xenografts of cervical cancer cell lines SiHa and ME180 were grown subcutaneously in SCID mice. Samples were obtained from these tumours with a 21 Gauge needle using a non-aspiration technique (Zajdela), and the resulting tissue plug was either expelled directly into formalin to obtain a cell block, or used for direct smears (Lowhagen). Smears were air-dried or wet-fixed (alcohol or formalin). After needle samples were taken the mice were killed and the tumours were excised and fixed immediately in formalin. The different samples were stained with phosphospecific antibodies for Stat3 and NFkappaB.

Results: PhosphoStat3 and phosphoNFkappaB showed a relatively homogeneous distribution throughout the viable tumor area. Phosphoepitopes were demonstrated in samples expelled directly into formalin and embedded into paraffin blocks. The staining intensity was similar to that of histological sections of the excised tumors. Directly smeared material, however, showed a loss of staining.

Conclusions: FNB of solid tumors may be useful in anatomic sites where large core needle biopsy is not possible or not well tolerated. Phosphoepitopes can be demonstrated in cytologic specimens of this type when the sample is formalin fixed for a cell block preparation. Slide based laser scanning cytometry may be used to estimate pathway activity before and after the application of molecular targeted agents.

1558 Utilization of Chromosome Y Chromogenic In Situ Hybridization (CISH™) To Detect Male Cells in Surgical Pathology Specimens
AS Silva, M Palau, MJ Merino. NCI/NIH, Bethesda, MD.

Background: Sexual chromosomes demonstration by in situ hybridization has long been described and most studies in humans use Fluorescence In Situ Hybridization (FISH). Detection of chromosome Y and chromosomes X signals in different tissues from female and male patients, can be utilize in tissue identification as well as for identification of donor cells in transplanted patients. CISH™ has been described to have some advantages when compared to FISH: morphology visualization in the context of tissue using brigthfield microscope; permanent signals, permitting storage of slides for long periods and lower costs. We evaluated the applicability of chromosome Y CISH in surgical pathology specimens.

Design: We performed chromosome Y CISH using SPoT-Light Chromosome Y Probe and SPoT-Light CISH Centromer Detection Kit (ZYMED), according to manufacture instructions, in formalin-fixed paraffin embedded (FFPE) tissue from surgical biopsies and autopsy samples. Different tissues from females and males were studied as well as one case of sex mismatched bone marrow transplantation. The presence of a single dot whose diameter was less than 5% of the diameter of the nucleus was interpreted as hybridization to a single chromosome Y centromere, indicating a male cell. No staining in all cells was interpreted as no hybridization and hence, absence of male cells.

Results: Samples from females showed no hybridization. Samples from males showed conspicuous hybridization,especially in epithelial cells. CISH™ of rectal biopsies from the sex mismatched bone marrow and MSC transplanted female patient showed hybridization in stromal and mononuclear cells in the lamina propria, and very rare hybridization in epithelial cells.

Conclusions: Chromosome Y CISH is a useful technique applicable in FFPE pathological specimens for tissue identification as well as identification of donor cells.

1559 Jak2V617F Mutation Detection by Asymmetric Fluorescence Real-Time PCR and Melting Curve Analysis
J Stefka, SN Reading, MS Lim, KSJ Elenitoba-Johnson. University of Utah, Salt Lake City, UT.

Background: Chronic myeloproliferative disorders (CMPDs) are clonal stem cell hematopoietic processes characterized by proliferation of megakaryocytic, erythroid and/or myeloid lineages. The non-chronic myelogenous leukemia CMPDs include polycythemia vera (PV), essential thrombocytemia (ET) and chronic idiopathic myelofibrosis (CIMF). These disorders exhibit similarities spanning clinical, morphological and molecular features. An acquired mutation in JH2 domain of Jak2 tyrosine kinase (JakV617F) has been identified in >95% of PV and about 50% of ET and CIMF. This mutation disrupts the auto-inhibitory effect of JH2 domain and renders affected stem cells relatively independent of growth factors. The mutational status of Jak2 could serve as an additional parameter to distinguish a CMPD from reactive processes and provide a future therapeutic target based on mutational status.

Design: DNA was obtained from HEL, an eyrthroleukemia cell line homozygous for the V617F point mutation in JAK2 tyrosine kinase gene. CMPD patient samples were obtained from bone marrow and wild-type JAK2 control DNA was extracted from placental tissue. Asymmetric real-time PCR using a fluorescien-labeled oligonucleotide (SimpleProbe®) was conducted on LightCycler 1.5 system (Roche Diagnostics) utilizing LightCycler DNA Master Hybprobe reaction mix. PCR products were subjected to cycle sequencing on ABI Prism 3100 system using Big Dye chemistry, (Applied Biosystems). Sequence data was analyzed using SeqMan II module (DNASTAR Inc.).

Results: The V617F mutation was detected at a sensitivity of 2.5% using the fluorescence PCR approach. Melting curve analysis successfully discriminated mutated from non-mutated alleles by the melting temperature (T_m) of the wild-type peak (T_m 65.73°C) and that of the mutant peak (T_m 58.75°C). Analyzed CMPD patient samples tested positive for Jak2 mutation in background of wild type Jak2. The presence of expected mutated and wild type Jak2 genotype (both G and T base present) was confirmed by sequencing.

Conclusions: Fluorescent melting curve analysis can be used as a rapid, sensitive and specific method to detect Jak2 mutational status. This can be used in conjunction with clinical and pathological criteria for diagnosis of a CMPD. Furthermore, presence of the mutation may identify patients for novel targeted therapeutic intervention.

1560 Evaluation of the ABI 7500 Fast Real Time PCR Instrument for Detecting Two Common Polymorphisms Associated with Hemochromatosis
LJ Tafe, DR Belloni, GJ Tsongalis. Dartmouth Medical School, Dartmouth-Hitchcock Medical Center, Lebanon, NH.
Background: Hereditary hemochromatosis is an autosomal recessive disorder characterized by abnormally increased iron absorption. The HFE gene, located at 6p21.3, contains two common single nucleotide polymorphisms (SNPs) C282Y and H63D, that are routinely tested for in the molecular diagnostics laboratory. Current technologies used to screen for these HFE SNPs include various modifications of the PCR and real time PCR technologies. In this study, we compared a new and improved ABI 7500 FAST real time PCR assay to a more traditional PCR-RFLP assay and an ABI 7700 real time PCR assay.
Design: In this study we utilized DNA samples from fifty-nine patients (clinicians wanted to confirm or rule-out hereditary hemochromatosis) who had been previously tested for the HFE SNPs using a PCR-RFLP assay and the ABI7700 real time PCR assay. DNA from all samples was isolated from whole blood using the PureGene Kit (Gentra, Inc. Minneapolis, MN) . All samples were previously tested using a PCR-RFLP assay and an ABI 7700 real time PCR assay with a MGB Eclipse ASR Probe system. The new assay utilized the following TAQman™ SNP Genotyping Assays: C_1085595 (C282Y) and C_1085600 (H63D) (ABI Assays-on-Demand) using ABI 2x fast universal master mix, 10-20 ng of genomic DNA in a total reaction volume of 10 μl using the default fast cycling conditions. A post amplification plate read was used for allelic discrimination according to the ABI 7500 user manual.
Results: Of fifty-nine samples, nine were homozygous for H63D, ten were heterozygous for H63D, seven were homozygous for C282Y, six were heterozygous for C282Y, six were compound heterozygotes, and twenty were wild type by all three assays. With the exception of one sample that was indeterminate by the TAQman™ SNP Genotyping Assay, all others showed 100% concordance between assays. This one sample was heterozygous for C282Y by the PCR-RFLP and ABI 7700 real time PCR assays, but there was an insufficient quantity of DNA to perform the TAQman™ SNP Genotyping Assay
Conclusions: Our study suggests that the ABI 7500 FAST TAQman™ SNP Genotyping Assay is comparable to the PCR-RFLP and ABI 7700 real time PCR methods in detecting and characterizing these two HFE SNPs. Improved software and thermocycling capabilities have resulted in a very robust TAQman™ assay that has the advantage of improved turn-around-time and throughput.

1561 Validation of Telepathology for Remote Frozen Section Evaluation of Pre-Transplant Donor Liver Biopsies
GA Talmon, SJ Radio, JL Wisecarver, JM Gulizia, K Bernal. University of Nebraska Medical Center, Omaha, NE.
Background: Frozen section biopsies of donor livers are commonly performed to evaluate the organ. The transmission of slide images via the Internet has the potential to reduce turnaround time or facilitate expert consultative review in remote locations. The purpose of this study is to correlate the frozen section diagnoses rendered via telepathology with those obtained by review of original glass slides.
Design: Forty consecutive liver allograft biopsies performed from June to November 2004 were obtained. Two liver pathologists independently and in a blinded fashion reviewed a representative frozen section slide from each case. These were graded using the criteria for organ acceptance: percent of macrovesicular fat present (10% increments), presence of periportal fibrosis (low grade: 0-2+, high-grade 3-4+), severity of chronic portal inflammation (0: none, 1: <2 foci of interface hepatitis, 2: at least two foci of interface hepatitis), and prominent cholestasis (present or absent). The slides were then randomized, scanned using the Trestle MedMicro system, and reviewed in a blinded fashion by the same pathologists.
Results: No case was judged to have high-grade fibrosis or prominent cholestasis at the time of original diagnosis. Combining the responses of the two reviewers, agreement between glass slides and scanned images was as follows: percent macrovesicular steatosis- 71/80 (89%, k=0.48), no value varying by more than 10%; fibrosis- 79/80 (99%, k=N/A); chronic portal inflammation- 63/80 (79%, k=0.43); cholestasis- 78/80 (98%, k=N/A). Interobserver agreement for each medium was as follows: steatosis- glass 35/40 (88%, k=0.53), scanned 36/40 (90%, k=0.46), no value varying by more than 10%; fibrosis- glass 40/40 (100%, k=N/A), scanned 39/40 (98%, k=N/A); inflammation- glass 33/40 (83%, k=0.55), scanned 31/40 (78%, k=0.35); cholestasis- glass 38/40 (95%, k=N/A); scanned 40/40 (100%, k=N/A). In this series, there would have been no change in the decision to accept an allograft on the basis of differing results obtained via the two methods.
Conclusions: There was good correlation between glass and scanned slides using commonly used criteria to determine organ acceptance. The variable that correlated the least was chronic portal inflammation, which also exhibited significant interobserver variability using both glass slides and scanned images. In no instance would an organ have been declined via telepathology that would have been found acceptable by examining the actual slides.

1562 In-Situ Gene Expression Profiling in Clinical Samples by Quantum Dot Based Multiplex Hybridization
E Tholouli, D Divizio, F O'Connell, D Twomey, R Levenson, JA Hoyland, JA Liu-Yin, CA Lee, TR Golub, M Loda, RJ Byers. Manchester Royal Infirmary, Manchester, United Kingdom; University of Manchester, Manchester, United Kingdom; Brigham & Women's Hospital, Boston, MA; Dana-Farber Cancer Institute, Boston, MA; MIT, Boston, MA; CRI, Woburn, MA.
Background: Gene expression profiling has identified many potentially useful prognostic gene signatures but there has been limited application to formalin-fixed, paraffin-embedded diagnostic biopsy specimens. We performed multiplexed in situ hybridization using quantum dot (QD)-labeled oligonucleotide probes to visualize

known expression signatures to biopsy specimens. Signals were detected and deconvoluted by spectral imaging.
Design: Streptavidin and amine coated QDs were coupled to oligonucleotide probes and used in automated in situ hybridization (ISH). Signal stability and ability to detect mRNA in archived tissue were assessed. As proof of concept, tissue specific oligonucleotide probes were utilized, to identify tumour types by spectral quantitation of specific probes / beta actin ratios. Finally, duplex ISH and triplex signal deconvolution was performed in single slides.
Results: Mcc10, a Clara cell specific gene, was restricted to the bronchiolar epithelium and myeloperoxidase (MPO) was present in AML and absent in ALL. Fluorescent signal was preserved over 18 months from the initial hybridization experiment while gene expression was detected in 30 year old prostatic cores. Tissue-specific probes (e.g. CDX2 and MITF) blindly identified recognized the appropriate tumor tissues. Duplex ISH was combined with IHC and triplex signal was successfully deconvoluted by spectral imaging.
Conclusions: We have demonstrated that QD labelled oligonucleotides can be successfully utilized in multiplex ISH in routinely processed clinical tissue. This will facilitate translational application of microarray identified gene signatures in the clinical setting with multiplexed probe detection.

1563 Development/Validation of a Comprehensive High Throughput Quantitative Assay for *BCRABL* Transcripts
JA Thorson, HC Weigelin, L Zhou, JK Howard. University of Michigan, Ann Arbor, MI; Case Western Reserve University, Cleveland, OH.
Background: Optimal management of chronic myeloid leukemia is increasingly dependent upon quantification of *BCRABL* transcripts. Accurate laboratory assessment of *BCRABL* transcript levels is complicated by the potential presence of fusion transcripts involving *BCR* exon 1 or *ABL* exon 3 which are not detected by many assays. Real time RT-PCR assays, which are commonly utilized by clinical laboratories, can accurately quantify transcript levels; however, detection limits are generally inferior to those of qualitative, nested RT-PCR assays. Our goal was to develop a high throughput assay for *BCRABL* transcript quantification capable of detecting multiple transcript forms and having a detection limit equal to that of our existing qualitative nested RT-PCR assay.
Design: RNA is reverse transcribed using an *ABL* antisense primer. Five real time PCR assays are performed simultaneously on each specimen in a micro-volume 384 well plate. Separate primer/probe sets are used to quantify *BCRABL* b2a2, b3a2 and *ABL* transcripts. Additional primer/probe sets detect *BCRABL* e1a2, e1a3, b2a3, and b3a3 transcripts. Samples are assayed in duplicate, with a maximum throughput of 24 samples per plate. Transcripts are quantified against plasmid standards and the ratio of *BCRABL* to *ABL* transcripts is calculated. Precision and accuracy were evaluated using dilutions of cell line RNA. Fifty clinical samples received for *BCRABL* determination were evaluated by real time RT-PCR and the results compared to those obtained from qualitative RT-PCR assays.
Results: A detection limit of 5 copies was obtained for each type of transcript. The intra-run CV was 4.3% overall. Inter-run CVs were 13% at 50,000 copies of *BCRABL* and 22% at 100 copies. By qualitative RT-PCR, 27/50 samples were *BCRABL* b2a2/b3a2+, 8/50 were e1a2+, and 4/50 were positive for b2a2/b3a2 and e1a2; 11/50 samples were negative for *BCRABL*. The real time RT-PCR assay demonstrated a 100% concordance with these results and also correctly typed one known b3a3+ sample.
Conclusions: We have developed a high throughput, high precision real time RT-PCR assay capable of quantifiying multiple *BCRABL* transcript forms. The detection limit of the assay is equivalent to that obtained with a nested RT-PCR assay. The ability to detect multiple transcript types coupled with a low detection limit allows comprehensive screening and minimal residual disease assessment to be performed in a single, economical assay.

1564 Comparison of 4 Scales for Quantifying Antigen Expression in Immunoperoxidase Stains: Assessment of Pathologist Agreement
LD True, S Hawley, A Herstein, JP Simko, L Fazli, J Virgin, EC Jones, BS Knudsen, AD Etzioni. University of Washington, Seattle, WA; Fred Hutchinson Cancer Center, Seattle, WA; University of California, San Francisco, CA; University of British Columbia, Vancouver, BC, Canada.
Background: Tissue biomarkers, using immunoperoxidase stains, play a critical role in stratifying patients by prognosis and by candidacy for systemic therapy and molecular therapy. As currently practiced, semi-quantitative estimates of expression levels of biomarkers are obtained by estimating the extent and intensity of immunoreactivity. Since immunoperoxidase stains are not stoichiometric and since assessments are made visually, we questioned the degree of agreement by pathologists in assessing immunostains.
Design: 30 primary prostate carcinomas immunostained for 2 antigens with potential prognostic power (MTA1 and MAOa) were evaluated independently by 6 pathologists using 4 methods of quantifying immunostains – binary (BIN: antigen present or absent in any tumor cells), 4-point (no staining, equivocal, moderate staining in a convincing number of cells, definitive), categorical (CAT: percentage of tumor cells staining at each of 3 intensity levels – none, faint, intense), and categorical composition (CC: staining in 0, <5%, 5 to 20%, or > 20% of tumor cells). The sequence of applying these 4 evaluation methods was randomized for each pathologist to control for "learning" bias. The percentage of cases per method and by pathologist that satisfied a current threshold for taking clinical action were recorded and compared.
Results: The pairwise agreement (the estimated percentage of cases for which pathologist A assigns the same rating as pathologist B) between pathologists was as follows: BIN: 47 to 93%, 4-pt: 47 to 97%, CAT: 73 to 100%, and CC: 50 to 90%. The general agreement for each method, i.e. the percentage of cases for which a randomly chosen pathologist

will agree with a second, randomly chosen pathologist, was as follows: BIN: 78%, 4-point: 76%, CAT: 88% and CC: 77%.

Conclusions: The range of overall agreement in immunohistochemical scoring using 4 conventional methods for quantifying stains was 76 to 88%. Agreement was best using the categorical method. However, since agreement was suboptimal for the individual patient , finding a more reproducible method of quantifying protein expression in tissue samples is needed to ensure that patients are managed in a manner appropriate to the phenotype of their tumors.

1565   Silver In Situ Hybridization (SISH); Validation of a Fully Automated *HER2* Staining Protocol
RR Tubbs, DG Hicks, JD Pettay, WC Powell, PC Roche, L Pang, EV Klohe, W Liu, RD Powell, JF Hainfeld, R Lounsbury, M Loftus, TM Grogan. Cleveland Clinic Foundation, Cleveland, OH; Ventana Medical Systems, Inc, Tucson, AZ; Nanoprobes, Inc, Yaphank, NY.

Background: Recent advances in enzyme metallography have enabled high-resolution ultrasensitive bright field detection of individual gene loci via interphase in situ hybridization which may be more easily adaptable to surgical pathology practice than FISH. However, practical application has been limited by manual components of the assay. We investigated the feasibility of globally automating enzyme metallography staining (Silver In Situ Hybridization, SISH™).

Design: 200 invasive breast carcinomas in tissue midi arrays (TMDA) were studied using unstained paraffin sections and automated *HER2* silver in situ hybridization (SISH™) (Ventana) using an automated staining workstation (Benchmark XT). All components of SISH™ were fully automated including deparaffinization, cell conditioning, enzyme pretreatment, probe application and hybridization, stringency washes, and counterstain. SISH™ results were evaluated using a conventional brightfield microscope without the use of oil immersion as follows: *HER2* not amplified = 1-2 signals in $\geq$ in 30% of tumor nuclei; (nonamplified presumed polysomic = 3-5 signals in $\geq$ 30% of tumor nuclei; and amplified ($\geq$ 6 signals per nucleus in > 30% of tumor nuclei.

Results: SISH signals were easily enumerated discreet, metallic silver deposits essentially identical to patterns observed for the same cases using FISH. No manual intervention was required during the entire in situ hybridization procedure - - slides were placed on the instrument and removed at the end of the automated instrument run time. Of 200 TMDA cores, 197 contained tumor that could be scored. Comparable signal separation between amplified and nonamplified cases was achievable with both FISH and SISH—the presence or absence of *HER2* gene amplification assessed by SISH™ was highly concordant with FISH (kappa = 0.911)l Furthermore, HER2 signal counts and HER2/CEP17 ratios obtained by FISH differed significantly between SISH amplified and nonamplified cases (p<0.0001; unpaired t test).

Conclusions: Globally automated silver in situ hybridization (SISH™) is an excellent bright field alternative to FISH and IHC for assessment of *HER2* status in breast carcinoma. This approach is readily incorporated into the workflow of the surgical pathology laboratory and the pathologist's professional interpretation.

1566   Specificity of Interphase FISH Probes for Detection of Sarcoma and Lymphoma Associated Translocations in Paraffin Sections Is Readily Assessed Using Tissue Microarrays Constructed from Murine Xenografts
RR Tubbs, JD Pettay, MB Hartke, T Barry, G Payne, PC Roche, M Loftus, E Swain, TM Grogan. Cleveland Clinic Foundation, Cleveland, OH; PhenoPath Laboratories, Seattle, WA; University of Arizona, Tucson, AZ; Ventana Medical Systems, Inc, Tucson, AZ.

Background: Implementation of interphase fluorescence in situ hybridization (FISH) assay in the clinical laboratory requires validation against established methods. Validation tools in common use include exchange of consecutive sections with another institution that has already established the FISH assay, confirmation of specificity using normal metaphases, comparison with conventional banded metaphase cytogenetics, consecutive paraffin sections of a validation set tested by a reference laboratory, and specificity assessment against well characterized cell lines. We investigated the feasibility of using tissue microarrays (TMA) constructed from murine xenografts as a preliminary specificity-screening tool for validation of interphase FISH assays according to protocols described by Ventana Medical Systems, Inc. (VMSI, Tucson).

Design: Ten cell lines currently in use for FISH controls were used to generate xenografts in SCID mice which were fixed in formalin and paraffin embedded and a TMA constructed. Xenografts reflected a wide range of translocations used routinely for formalin fixed paraffin embedded sections evaluated by FISH. FISH probe cocktails (Abbott-Vysis), for the following translocations were used in this study: t(11;14) (fusion format) and EWS, CMYC, and IGH (breakapart format). On-line deparaffinization, cell conditioning, and prehybridization steps were performed both manually and were also automated using a staining workstation (Ventana Discovery XT™); hybridization and stringency washes were performed manually offline. FISH-stained TMAs were tracked using a Metasystems image scanner, and subjected to classifiers specifically developed for each molecular abnormality. Results were then correlated with the established genotype for each parent cell line.

Results: The FISH results for each xenograft in the TMA corresponded exactly to the genotype established for the parent cell line from which the xenograft was prepared.

Conclusions: Moderate complexity tissue microarrays constructed from murine xenografts are an excellent validation tool for initial assessment of interphase FISH probe specificity.

1567   Genotyping of Phenotypically Defined Cells: Enhanced ImmunoFISH Tyramide Signal Amplication (TSA) Protects Immunophenotypically Defined Populations for Gated Genotyping
RR Tubbs, K Das, E Swain, R Lounsbury, JR Cook, JD Pettay, PC Roche, TM Grogan. Cleveland Clinic Foundation, Cleveland, OH; Ventana Medical Systems, Inc, Tucson, AZ.

Background: Stromal and vascular interactions within malignant neoplasms have gained importance in understanding tumor growth and progression. Understanding the complex mechanisms of gene expression and their aberrations are important in deciphering the mechanisms of disease progression and the potential for therapeutic intervention. Tools for simultaneously visualizing the immunophenotype and genotype exist, but are frequently hampered by a delicate balance between removing sufficient protein that prevents access of the probe to target nucleic acids, and preserving sufficient target antigen for immunophenotyping. The result is often suboptimal, with either suboptimally visualized gene deletions or amplifications due to persistent masking protein, or over digestion of the protein target.

Design: Using the proliferating endothelial cell compartment within glioblastoma multiforme, we tested the hypothesis that tyramide signal amplification could be used to "protect" the target antigen during immunophenotyping, while still permitting sufficient protein digestion to guarantee probe accessibility to nucleic acid target. Validation was done using a single TMA containing 30 glioblastoma multiforme cases previously genotyped for EGFR amplification using the dual-color CEP7/EGFR probe set (Abbott/Vysis). All staining steps exclusive of hybridization and stringency washes were automated using an in situ hybridization workstation (Ventana Discovery XT). Signal enumeration was done on a FISH imaging workstation (MetaSystems). The ability of the FISH staining system to segregate endothelial cells from tumor cells for genotyping was assessed qualitatively; EGFR amplification was assessed by a customized CEP7/EGFR classifier.

Results: Deposition of the Alexafluor dye was not altered by enzyme pretreatment. Excellent delineation of endothelial cells, and their separation from tumor cells, was achieved using this novel approach. The correlation between EGFR/CEP7 amplification ratios comparing manual to automated scoring was excellent.

Conclusions: Genotyping of phenotypically defined cells using enhanced immunoFISH tyramide signal amplification protects immunophenotypically defined populations for successfully gated genotyping.

1568   Comparison of Cell Block Methods for Non-Gynecologic ThinPrep Specimens
Z Tynski, JK Wasman, FW Abdul-Karim, N Wang. Case Western Reserve University, Cleveland, OH.

Background: Various cell block (CB) methods have been proposed for ThinPrep (TP) Pap specimens including the recently described Inverted Filter Sedimentation (IFS). The purpose of this study was to compare 4 CB methods in the setting of non-gynecologic TP specimens, assessing each for cellularity, quality of CB, ease of preparation, and utility for immunohistochemical (IH) staining.

Design: Forty-eight cell blocks were prepared from 12 non-gynecologic TP specimens. Each specimen was collected into 30cc of Cytolyte: 9 fine needle aspirates obtained from surgical specimens (4 thyroid nodules, 1 lung mass, 2 lymph nodes, 1 breast mass, 1 liver mass), 2 pleural fluids, and 1 ascites fluid. Each specimen was divided equally into 4 tubes; each tube was centrifuged and its supernatant discarded. Three drops of cell sediment from each tube was added to PreservCyt and a TP slide was generated for each tube to assess cellularity and to ensure that specimens were equally divided. CBs were prepared from the remaining cell sediment using 4 CB methods: (1) IFS: Cell sediment and residual PreservCyt fluid were filtered through the inverted TP filter, which was then removed from the cylinder and submitted for processing (2) Thrombin method: Plasma and thrombin were added to form a clot (3) Albumin method: Albumin and 95% ETOH were added to form a precipitate (4) Simple sedimentation: Cell sediment was placed in Histowrap. Each CB was given a cellularity score: 0 no cells, 1+ hypocellular, 2+ hypocellular but with tissue fragments, 3+ cellular. Three IH stains were performed for each of the thrombin and albumin CBs.

Results: A cellularity score of 2+ or 3+ was given for 11/12 thrombin, 7/12 IFS, 5/12 albumin, and 2/12 simple sedimentation CBs. Thrombin CBs demonstrated a pale background clot which did not interfere with cellular detail; cells and cell fragments were evenly distributed. Albumin CBs had a distracting dense pink background and sections were frequently uneven and folded. IFS CBs had a clear background, however cells appeared artifactually crowded. Only the IFS method was difficult to master and added significant time to processing. All thrombin and albumin CBs demonstrated appropriate IH staining.

Conclusions: In the setting of non-gynecologic TP specimens, the thrombin method produced the best CB in regards to cellularity, cell distribution, and background quality. The thrombin CB was easily prepared and demonstrated appropriate IH staining. The IFS technique, while specific to TP, was difficult to perform and produced a less optimal cell block.

1569   Fully Melting of Tissue Microarrays Using a Stabilization Body
UF Vogel, BD Bueltmann. University Clinic, Eberhard-Karls-University, Tuebingen, Baden-Wuerttemberg, Germany.

Background: Paraffin tissue microarrays (PTMAs) are blocks of paraffin with up to 1000 paraffin tissue core biopsies (PTCBs). The construction of PTMAs consists of putting PTCBs from so-called donor blocks into preformed holes of a so-called recipient block (PTMA). These holes can be made by punching, pouring with a spacer or by drilling. At sectioning, the problem may occur that some PTCBs fold up when the section floats on the water. This may be due to an insufficient contact of the paraffins of the PTCBs and the recipient block. Mengel et al. (MaxArray-technique) solved this problem by melting the PTMA block in a two-step melting procedure (Lilischkis R ,

von Wasielewski R, Mengel M: Method for production of material blocks with multiple test samples. PCT International Publication Number: WO 01/51910 A1. 2001. International Patent Number: PCT/DE00/04647). To simplify this melting procedure by reducing it to one-step and to overcome restrictions of the MaxArray-technique concerning equipment and PTMA design we looked for a new technique.
Design: As recipient blocks (PTMAs) we used stabilization bodies (i.e. paraffinized biological material (e.g. liver tissue, lung tissue), blocks of paraffinized agar and synthetic spongy material (e.g. packaging material, sponges for cleaning)) cast in routine paraffin blocks. Prior to drilling the holes as presented previously, the later PTMAs were carefully trimmed in order to have the stabilization bodies reach the surface of the PTMA. After filling the holes with PTCBs, the PTMAs were put into routinely used steel embedding molds, put on a hot plate and heated up to 65°C. After fully melting the paraffin the steel embedding molds with the PTMAs were cooled down and processed routinely.
Results: The different materials used as stabilization bodies showed different properties at paraffinizing, drilling, melting and cutting. The best results were achieved with biological tissues. The folding and the detachment of the PTCBs was significantly reduced by creating a solid contact between the paraffins of the PTMA and the PTCBS. The stainings, especially the immunohistochemical reactions, did not show any deterioration due to the melting process. Well-known problems of paraffin sectioning like the disruption of sections were not solved by melting a PTMA after filling.
Conclusions: By using stabilization bodies a one step fully melting of the PTMAs is possible without the need for a special equipment and without any limitations concerning the number and the diameter of the holes of a PTMA.

1570   Depositing Archived Paraffin Tissue Core Biopsies in Paraffin Tissue Microarrays by Using a Paraffin Tissue Punch with a Countersunk
UF Vogel, BD Bueltmann. University Clinic, Eberhard-Karls-University, Tuebingen, Baden-Wuerttemberg, Germany.
Background: Paraffin tissue microarrays (PTMAs) as introduced by Kononen et al. in 1998 became a widely used technique in routine pathology and especially in research. By the use of a tissue puncher/arrayer (Beecher Instruments, USA), Kononen took paraffin tissue core biopsies (PTCBs) of 0.6 - 2 mm in diameter from routine paraffin tissue blocks and transferred them to another paraffin block with up to 1000 holes. However, till now archived PTCBs can not be used by the system of Kononen for the construction of PTMAs in contrast to the techniques as described by Wan et al. and Mengel et al.. In order to use archived PTCBs for PTMAs constructed with the most popular Beecher system we looked for a technique to overcome this drawback.
Design: We modified the commercially available Beecher paraffin tissue punch by applying a countersunk in the upper opening. To test this new punch PTCBs were punched out of routine paraffin tissue blocks and stored in Eppendorf tubes. Then PTMAs were constructed according to routine procedures. However, instead of punching the PTCBs, the PTCBs were transferred from the microtubes to the countersunk of the Beecher tissue punch using a tweezers. With the stylet, the PTCBs were further pushed into the punch and finally pressed into the holes of the PTMAs. After filling the holes, the PTMAs were cut and the sections processed according to routine procedures.
Results: We could construct PTMAs with up to 322 archived PTCBs. Seldom the PTCBs broke when they were handled with the tweezers or the stylet. The time to fill a PTMA with stored PTCBs was similar to PTMAs constructed with immediately punched and inserted PTCBs despite of the procedure of picking up the PTCBs with the tweezers.
Conclusions: By applying a countersunk to the tissue punch the insertion of archived PTCBs into the tissue punch is facilitated. Thus, the construction of PTMAs consisting of formerly archived PTCBs is possible by using the widely distributed Beecher System.

1571   Flow Cytometric Analysis of Vβ Repertoire for Assessing T-Cell Clonal Proliferations
EX Wei, DM Veillon, JD Cotelingam, ML Nordberg. Louisiana State University Health Sciences Center, Shreveport, LA.
Background: T-cell lymphoproliferative disorders have features of T-cell subset restriction, aberrant CD4/CD8 ratio, antigen loss or inappropriate expression. Molecular analysis targeting T-cell receptor (TCR) gene rearrangements by PCR is commonly used to determine T-cell monoclonality. Flow cytometric assessment of TCR using TCR β-chain variable regions (TCR-Vβ) emerges as an alternative way to traditional molecular techniques.
Design: T-cell analyses were performed on sixty five patient specimens by conventional flow cytometry. TCRβ, γ and/or δ gene rearrangements (InVivoscribe Technologies, San Diego, CA) were assayed by PCR and ascertained using capillary gel electrophoresis. Selective patients with TCRαβ T-cell proliferations were evaluated for clonal Vβ repertoire. Flow cytometry for monoclonal TCR-Vβ expression were performed using IOTest Beta Mark TCR-Vβ Repertoire Kit (Beckman Coulter, Miami, FL). Cases chosen include T-ALL, T-cell large granular lymphocytic leukemia, hepatosplenic T-cell lymphoma and other T-cell lymphoproliferative disorders. Analyses were performed using 5-parameter, 4-color immunophenotyping with incorporation of CD3 gating. Clonal expansions were quantified with established criteria and examined with EXPO software (Beckman Coulter).
Results: Twenty-eight (43%) patient specimens demonstrated clonal gene rearrangements by PCR assays. Twenty specimens positive by PCR showed monoclonality with TCR-Vβ analyses by revealing a predominant Vβ subpopulation, or most T-cells nonreactive with any Vβ antibodies; other cases, however, demonstrated only suspicious or non-clonal flow cytometry results. Suspicious cases tended to have substantial restrictions of T-cell subpopulations. Non-clonal specimens by TCR-Vβ expression had very low abnormal circulating lymphocytes, below the threshold of detection. Two cases of reactive T-cell proliferation in autoimmune disorders showed clonal Vβ repertoire.

Conclusions: TCR-Vβ expression by flow cytometry serves as an attractive addition to multicolor, multiparameter immunophenotyping. It has advantages of rapid turnaround time, convenient T-cell subset studies and quantitative results. Even though less sensitive than PCR, this approach may be used as an initial screening for T-cell monoclonality, particularly in laboratories without immediate access to molecular analyses. The particular Vβ+ T-cells can be monitored during chemotherapy once that subpopulation is identified. The limitations may be the expenses and suboptimal sensitivity.

1572   Analysis of T-Cell Clonality Using Laser Capture Microdissection and High Resolution Microcapillary Electrophoresis
E Yakirevich, CL Jackson, P Meitner, D MacKenzie, L Robinson-Bostom, MB Resnick. Rhode Island Hospital and Brown Medical School, Providence, RI.
Background: Polymerase chain reaction (PCR)-based analysis of T-cell receptor (TCR) gene rearrangements is a useful method in the diagnosis of lymphoproliferative disorders. Identification of a clonal lymphocytic population may be difficult because of the paucity of the infiltrate as well as a heterogeneous population of cells. The aim of this study was to assess the diagnostic utility of LCM and high resolution microcapillary electrophoresis in the clonality analysis of small biopsy specimens.
Design: Clonality was assessed in 24 cases, including five reactive tonsils, five reactive lymph nodes, six inflammatory skin lesions, and eight T-cell lymphomas (three nodal and five cutaneous). CD3 positive T-lymphocytes were captured by LCM (Arcturus) from paraffinized IHC stained sections. Genomic DNA was extracted from the microdissected cells as well as from the whole tissue sections and subsequently analyzed for TCR-γ gene rearrangement by PCR. PCR products were detected using high resolution microcapillary electrppohoresis with the DNA 500 LabChip and Agilent Bioanalyzer.
Results: For LCM, numbers of cells varying from 10-10,000 were captured. We determined that 10 captured cells were sufficient to obtain a PCR product in the TCR-γ gene rearrangement assay using non-nested PCR. TCR-γ gene rearrangement analysis revealed monoclonal bands when the cell number was between 10 to 1,000 cells in reactive tonsils, lymph nodes, and inflammatory skin infiltrates. This pattern changed to polyclonal when higher numbers of cells were microdissected (2,000 to 10,000 cells). In contrast, LCM captured lymphoma cells were constantly monoclonal whether low or high numbers of cells were microdissected. The monoclonal peaks from LCM were identical in base pair size to those from the whole section extracts. Microcapillary electrophoresis coupled with LCM provided improved diagnostic sensitivity. In two of eight lymphoma cases, LCM revealed diagnostic monoclonal bands, whereas routine TCR-γ assessment of whole tissue sections with 10% polyacrylamide gel electrophoresis demonstrated only minor clonal bands.
Conclusions: Clonality determined by LCM is cell number dependent. We conclude that biopsy specimens containing low number of reactive polyclonal T-cells (less than 2,000 cells) may produce pseudomonoclonal bands and these cases should be interpreted with great caution. LCM coupled with microcapillary electrophoresis results in higher sensitivity and facilitates TCR-γ gene rearrangement analysis.

Ultrastructural

1573   Pediatric and Adult Hepatic Embryonal Sarcoma: A Comparative Ultrastructural Study with Morphologic Correlations
NP Agaram, A Baren, CR Antonescu. Memorial Sloan-Kettering Cancer Center, New York, NY.
Background: Hepatic embryonal (undifferentiated) sarcoma (ES) is a rare pediatric tumor occurring predominantly in the first decade of life, but few examples of adult ES have been also described. Isolated ultrastructural reports describe contradictory lines of differentiation in these tumors. The objective of this study is to identify the distinctive ultrastructural features of ES in both pediatric and adult age groups and to correlate the findings with morphology.
Design: Four pediatric and 3 adult ES cases with available Electron Microscopic and Pathologic material were identified. The morphologic features analyzed included cell type, presence of giant cells, nuclear pleomorphism, cytoplasmic content, eosinophilic globules, necrosis, and presence of inflammation. The ultrastructural findings recorded were cell type, presence of secondary lysosomes with dense precipitates, RER and mitochondria morphology, intracytoplasmic fat droplets and cytoplasmic filaments.
Results: Morphologically, all cases showed plump to spindle cells, bizarre giant cells, eosinophilic globules and necrosis. In 5 cases areas of myxoid stroma and inflammatory cells were noted. Ultrastructurally, the hallmark features in all 7 cases included sequestered and dilated RERs and secondary lysosomes with dense precipitates. Dilated mitochondria were seen in 6/7 cases, and in 3 mitochondrial-RER complexes. Other features included intracytoplasmic fat droplets (5/7), scant actin microfilaments (3/7), and focal glycogen pools (2/7). In 4/7 cases, small undifferentiated cells with minimal amount of cytoplasm and cellular organelles were also identified.
Conclusions: Hepatic ES have distinctive ultrastructural findings, including dilated sequestered RER and dense lysosomal precipitates, which correlate with the eosinophilic hyaline bodies seen microscopically. These findings suggest that ES are composed of fibroblastic, fibrohistiocytic and undifferentiated cells. Other lines of differentiation were not identified in this series. The pediatric and adult ES show similar morphologic and ultrastructural features.